Response to Anonymous Referee #1

We thank the reviewer for the constructive suggestions/comments. Below we provide a point-by-point response to individual comments (comments in italics, responses in plain font; page numbers refer to the ACPD version; figures used in the response are labeled as Fig. R1, Fig. R2,…).

Comments and suggestions:

Authors basically reported the number concentrations of FAPs as FLx, where x is channel number. As shown as figures (e.g., Fig. 6), some FLx particles have a significant fluorescent intensity at a channel other than x. It is expected that the sum of FL1, FL2, and FL3 concentrations can exceed those of all FAPs (somewhat confusing). As WIBS has a function to detect wavelength-band fluorescence, the observed data sets can create automatically seven types (= 2^3- 1) of FAPs, where there is no overlap. Perring et al. (2015) presented this approach as authors also did as a part of the results. I recommend removing the descriptions on FLx typology and rearranging the data analysis of the seven-type FAPs at the first step to interpret how the FAPs concentrations varied during the observation period. This can improve the readability of the manuscript.

Responses and Revisions:

Good suggestion. In this study, we firstly reported the FAPs as FLx because this is the traditional method used in previous studies (Gabey et al., 2011; Healy et al., 2014), and the results can hence be comparable. However, as the referee suggested, we realized that it is a better way to focus on this seven-type instead of the FLx. Therefore, we have rearranged the structure of our paper:

In section 3.1, we will briefly report the number concentration of FLx and compare with previous studies, and their correlations with BC mass fraction are also introduced.

In section 3.2, we will show the classification of seven-type and analyze the number size distributions and diurnal variations.

Comments and suggestions:

Authors suggested the presence of "some other fluorophores" through the discussion on the comparison between non-combustion related FAPs at Nanjing and FAPs observed in other different "clean background" areas. As the atmospheric environment, ecosystem, human activities, and some other factors can greatly affect the emission of bioaerosols, the concentration levels of bioaerosols can be different

among places and not be necessarily same. To the best of my knowledge, no one knows the true values of bioaerosols concentrations at Nanjing. If there is no evidence to support this message, authors should remove this sentence and modify the sentence line 322-325.

Responses and Revisions:

In principle, the number concentration of bioaerosols is assumed to be higher in rainforests like Amazon and Borneo, being dominated by the biological activities. A previous study in Nanjing (Wei et al., 2015) also reported lower bioaerosols loading of 0.04 cm^{-3} on average, although the result might not be representative due to the different instrument (UV-APS) applied and the limited sampling time (2.3 hours). We therefore hypothesize that our observation is influenced by non-biological substances. We have revised this sentence:

"The number concentrations of the identified two types of bioaerosols (0.66 cm^{-3} for type C and 0.64 cm^{-3} for non-combustion-related type), however, were still higher than those observed in clean background areas and in the previous study in Nanjing (Wei et al., 2015), indicating they may also include some other non-biological fluorophores, such as dusts."

Comments and suggestions:

Authors only classified FL3 (type C, BC, AC, and ABC) particles into non-combustion related (NCR) and combustion-related (CR). Although type A, B, and AB particles, which consist of a large part of all FAPs, they are not included in the classification. Why did authors use only the fluorescent intensity at channel 3 (I3)? A simple way to see the correlation coefficient between specific type FAPs and BC/PM ratios suggests that type A and AB (type B) should be categorized into CR (NCR). If authors use only I3 information, they do not need to deploy WIBS, and simply should do UV-APS which has almost the same function. It is pity that important and useful information is not included in the data analysis presented in this paper.

I recommend as follows.

Please explain the benefits to deploy WIBS instead of UV-APS at Nanjing in this study if you use only I3 for the classification of FAPs.

A large fraction of FAPs, type A, B, and AB, should be considered and included into the classification.

Responses and Revisions:

The advantage of WIBS is in the 2×2 excitation (280 nm and 370 nm) and emission (310-400 nm and 420-650 nm) matrix, which provides additional dimensions of data evaluation. That's the reason why we used it in this study. Our analysis focused on

FL3 channel because this channel has been validated against other independent method. For example, Huffman et al., (2012) showed the relative placement and proportion of PBAP from SEM (scanning electron microscopy) analysis were very similar to that of PBAP from UV-APS in Amazon rainforest. The good agreement (R^2=0.78) between FL3 channel (WIBS) and UV-APS was also reported (Healy et al., 2014). We are not aware of similar validation for the other channels under ambient conditions. However, we followed the referee's suggestion to demonstrate the seven-type classification in the revised manuscript and included the similar analysis for I_{FL1} and I_{FL2} in the supplement.

Comments and suggestions:

PAHs emitted with BC through the incomplete combustion are originally in gas phase and subsequently can be scavenged by the preexisting surface of aerosol particles. Therefore, BC is one the carriers of PAHs. It is the fact that almost all of PAHs share the emission sources with BC. However, all the particles associated with PAHs cannot be combustion-generated, are just combustion-related. I recommend modifying the terminology of "combustion-generated".

Responses and Revisions:

Suggestion approved. We replaced "combustion-generated" by "combustion-related" in the revised manuscript.

Comments and suggestions:

Authors analyzed in detail the size-dependence of FL3 fraction classified by I3. To the best of my knowledge, Figure 9 is one the most important results in this study. Positive correlation of BC/PM and FL3 fraction was clear for the size range of 1-2 μm. I have some questions on the interpretation of the results as follows.

How did authors set the threshold value of I3, Icri? I'm confusing to see some findings in Figure 9 such as that the FL3 fraction for the size range of 4-5 μm with I3 > 18 was very weakly correlated with BC/PM and that the FL3 fraction for the size range of 5-15 μm with I3 > 18 (< 80) was positively but very weakly correlated with BC/PM. The former suggests the FL3 fraction for the size range of 4-5 μm with I3 > 18 can include the CR particles. The latter does that the FL3 fraction for the size range of 5-15 μm with 18 < I3 <80 can include the NCR particles. Especially, I could not understand that authors identify the FL3 particles for the size range of 5-15 μm with 18 < I3 <80 as CR particles. Please describe or guess what such huge combustion-related particles are. If not, we, the readers of this paper, will be confused.

Responses and Revisions:

In this study, we adopted the $M_{BC}/PM_{0.8}$ to assist the determination of I_{cri} because bioaerosols and combustion-generated FAPs are of different origins. Different I_{cri} values were scanned until the corresponding FAPs (intensity > I_{cri}) fraction showed a non-positive correlation with $M_{BC}/PM_{0.8.}$

We calculated the correlation coefficient for each I_{cri} in different size ranges. In practice, the correlations for these two groups of aerosol particles (4-5 μm, I_3>18 and 5-15 μm, 40 >I_{FL3}>18) are actually quite different. As shown in Fig. R1, a stronger correlation was found for the particles in the size range of 5-15 μm (R^2=0.98) than for particles in the size range of 4-5 μm (R^2=0.43). Thus we assume the particles in the size range of 4-5μm with I_3>18 are NCR particles.

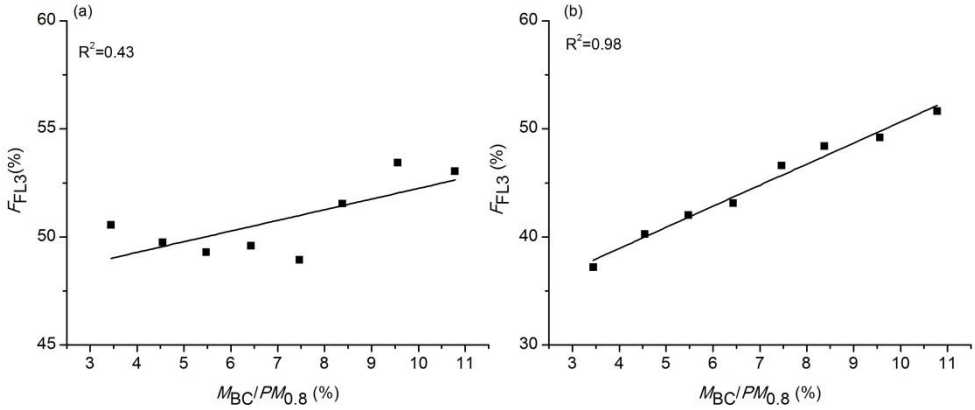

Figure R1. Correlations between FL3 fractions and $M_{BC}/PM_{0.8.}$ (a) Particles in the size range of 4-5 μm with I_{FL3}>18. (b) Particles in the size range of 5-15 μm with 40 >I_{FL3}>18.

Figure R2 shows the particle number size distributions from different sources. Our measurements revealed a coarse mode (D >1 μm) pattern that is similar to biomass burning particles (Hungershoefer et al., 2008). Both of them are dominated by the particles in the size range of 1-2 μm, with the fractions of 90% and 80% of the total number concentrations, respectively. On the contrary, particles from diesel vehicle emissions (Morawska et al., 1998) showed a different distribution in the coarse mode, and the contribution of particles in the size range of 1-2 μm was only 37%. Pöhlker et al. (2012) reported that interferent like PAHs, is particularly enriched on the surface of soot particles from biomass burning. Therefore a possible origin of these CR particles might be biomass burning.

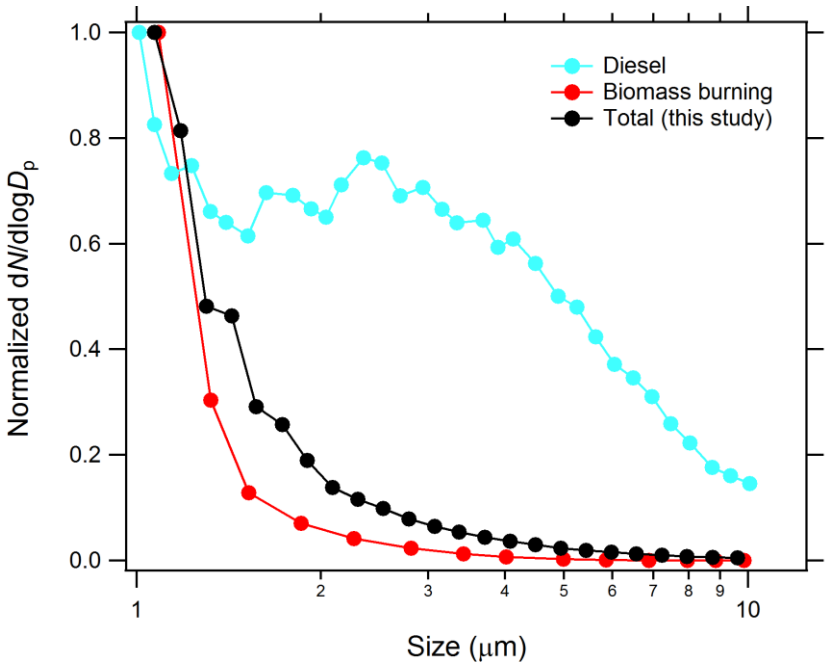

Figure R2. Comparisons of particle number size distributions from different sources.

Comments and suggestions:

In the section 3.1, authors showed the presence of CR particles which are FL2-related (type B, AB, BC, and ABC) and have the size of 4-5 μm. As the size ranges of CR particles defined in the section 3.3.2 were limited to 1-2 μm and 5-15 μm, the definition is inconsistent with the fact shown in the section 3.1. This can confuse the reader of this paper. Please recheck the assumptions and results and make the descriptions clearer.

Responses and Revisions:

The number size distribution of FL2 channel showed a peak at 3-4 μm, which was mainly contributed by type B particles (58%, Fig. R3b). Meanwhile, this peak showed a good correlation with $M_{BC}/PM_{0.8}$ (r=0.58). Therefore, the CR particles in FL2 channel actually indicated type B particles in 3-4 μm. We have included this info in the revised manuscript.

For the FL3 channel, there was no positive correlation between particles in the size range of 3-4 μm and $M_{BC}/PM_{0.8}$. We hence assigned these particles to NCR particles, which is different from FL2 channel. Also the good correlation suggested that the dominate CR particles are located between 1 and 2 μm in FL3 channel (r=0.82).

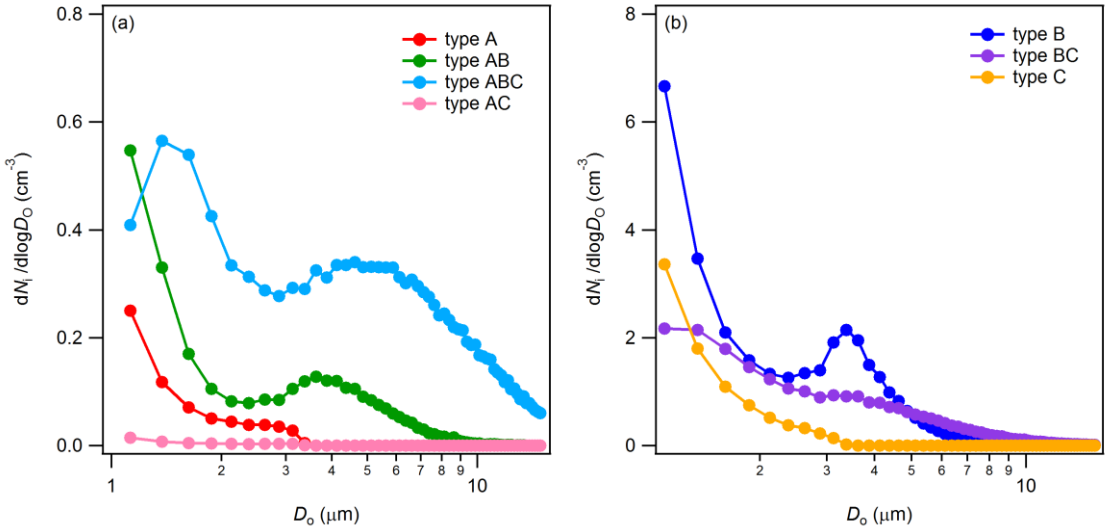

Figure R3. Mean number size distributions of (a) type A (red), type AB (green), type AC (pink) and type ABC (light blue); (b) type B (blue), type BC (purple) and type C (dark yellow).

Comments and suggestions:

Introduction: Line 56-57: Some of microorganisms cannot be cultivated. Please include this factor in the Introduction.

Responses and Revisions:

Suggestions approved. We have added this in the revised paper:
"These methods are time-consuming and their results may differ depending on the cultivation condition and procedures, especially considering the ubiquity of microorganisms that cannot be cultivated (Oliver, 2005; Pöhlker et al., 2012)."

Comments and suggestions:

Line 60-74: This paragraph is lengthy. Some details of the technical specification of commercial are not necessarily included in "Introduction" and those of WIBS should be moved into the experimental section. Why did authors include only the commercial one? Some custom-made UV-LIF instruments have ever been developed in previous studies such as Pan et al. (2009; 2011), Taketani et al. (2013), and Miyakawa et al. (2015). For the purpose to introduce the previous studies, authors should include more widely the UV-LIF techniques.

Responses and Revisions:

We have modified this in the revised paper:
"Since most biological materials contain fluorophores, instruments based on the

fluorescence detection, such as UV-APS (Ultraviolet Aerodynamic Particle Sizer; Brosseau et al., 2000), WIBS (Wideband Integrated Bioaerosol Spectrometer) and other custom-made instruments based on LIF (laser/light induced fluorescence) technology (Pan et al., 2009; Taketani et al., 2013; Miyakawa et al., 2015) have recently been developed for automatic online measurements of PBAPs..."

Comments and suggestions:

Instruments: What is the upper limit of the particle number concentrations that WIBS-4A can accurately measure? Based on OPC-like techniques, very high concentrations can affect the counting efficiency through the coincidence error. Please clarify whether WIBS-4A works well in such highly polluted region.

Responses and Revisions:

WIBS-4A can measure particles up to ~2×10^4 L^{-1}. Our measurements showed that the number concentration of FAPs was ~ 1.5×10^4 L^{-1} in Nanjing, which is within the upper limit. Meanwhile, the results showed a good agreement between WIBS and APS（R^2=0.9）at another polluted regional site around Beijing, indicating its application in highly polluted regions.

Comments and suggestions:

Line 144-146: The "ratio" approach can minimize the effects of some processes such as diurnal variations of PBL height and air mass dilution. To the best of my knowledge, this should be valid assuming no additional formation and loss process for both numerator and denominator species. Please clarify whether this assumption is valid.

Responses and Revisions:

The effects of variations of PBL height and air mass dilution should be similar for all kinds of species. For example, if we assume the values of M_{BC} and $PM_{0.8}$ are A and 10A, respectively. The mass fraction of BC ($M_{BC}/PM_{0.8}$) was 10% (A/10A=10%), and this fraction won't change due to the effect of PBL dilution in the case of no additional formation/loss processes for BC and fine particles. However, if there is a combustion source nearby, which can contribute the same additional amount of BC (A). Then the value of $M_{BC}/PM_{0.8}$ is 18% ($\frac{A+A}{10A+A}=18\%$), and this enhancement can reflect the combustion emission process. In other words, the additional source will strongly influence the numerator, while the denominator won't change a lot, resulting in the significant variation of ratio (relative fraction). Back to our case, we compared

the number fraction of FAPs with $M_{BC}/PM_{0.8}$, which both minimize the PBL influence, and the good correlation indicates a large contribution of combustion-generated aerosols to FAPs.

Comments and suggestions:

Line 184-195: Miyakawa et al. (2015) did not use similar technique. They used a multivariate analysis of the temporal variations of number concentrations of 8 type FAPs. This sentence is very confusing. This previous study should be included in "Introduction", because the results shown there closely relate to this study.

Responses and Revisions:

We have now included this technique in the introduction:
"Since most biological materials contain fluorophores, instruments based on the fluorescence detection, such as UV-APS (Ultraviolet Aerodynamic Particle Sizer) (Brosseau et al., 2000), WIBS (Wideband Integrated Bioaerosol Spectrometer) and other custom-made instruments based on the LIF (Laser induced fluorescence) technology (Pan et al., 2009; Taketani et al., 2013; Miyakawa et al., 2015), have recently been developed for online measurements of PBAPs."
The data analysis method has now been included in section 3.1:
"Miyakawa et al. (2015) had used factor analysis based on carbon monoxide, elemental carbon and other markers (using concentration instead of ratio) to identify "combustion-type" and "dust-type" aerosols in urban areas."

Comments and suggestions:

Line 200-212: Please clarify what fluorescent compound I and II are. Are they representative compound for the combustion- and non-combustion-related aerosols? Unless they are, I have an impression that authors picked up some compounds to well account for the observation results.

Responses and Revisions:

Compound I and II are tryptophan and pyrene, respectively. The former one is an amino acid (biological compound) and the latter one belongs to the group of PAHs (combustion-related compounds). In principle, we preliminarily distinguish compounds according to their disparate excitation-emission matrix profile.

Comments and suggestions:

Line 213-230: As noted in "Major comments", if you use only I3 signal, the information on type A, B, and AB particles should be ignored. Please consider some modification to the approach (See the "Major comments" for details).

Responses and Revisions:

We now have added FL1 and FL2 channel classification in the supplement.

Comments and suggestions:

Some sentences should be modified according to the revision. The last paragraph should be removed or moved to the discussion part, because all the descriptions are speculative, not suggested solely based on this study, and should not be discussed in Summary.

Responses and Revisions:

The last section of the last paragraph includes some conclusive remarks based on the findings (observations and data retrieval/evaluation methods) of our study, constraining current technical shortcomings and perspective. We think this is well suited in the conclusions. This way, we now re-titled this section as "Conclusions".

Comments and suggestions:

Line 63-64: UV-APS use the UV-laser for exciting the particles, so here UV-Laser induced fluorescence (UV-LIF) is correct.

Responses and Revisions:

Corrected.

Comments and suggestions:

Line 79: Miyakawa et al. (2015) deployed a custom-made UV-LIF instrument (not UV-APS and WIBS).

Responses and Revisions:

We now better explicate in the revised manuscript:
"Since most biological materials contain fluorophores, instruments based on the fluorescence detection, such as UV-APS (Ultraviolet Aerodynamic Particle Sizer; Brosseau et al., 2000), WIBS (Wideband Integrated Bioaerosol Spectrometer) and other custom-made instruments based on the LIF (laser/light induced fluorescence) technology (Pan et al., 2009; Taketani et al., 2013; Miyakawa et al., 2015) have recently been developed for automatic online measurements of PBAPs…."

Comments and suggestions:

Line 107: Is the silica gel dryer TSI's one or custom-made? If this is TSI's one, particle transmission efficiency for the coarse mode particles is not so good depending the sampling flow rate. If custom made, please clarify how authors locate it in front of WIBS-4A. The direction of flow in the dryer should be parallel to the sampling line.

Responses and Revisions:

The silica gel dryer is custom-made. It was installed vertically above the WIBS-4A. So the particle loss due to the gravity settling can hence be neglected. In the revised manuscript, we have clarified this:
"A 0.75 inch stainless-steel tube inlet was installed ~3 m above the roof, and sample air was dried by a vertical silica gel drier prior to entering the WIBS."

Comments and suggestions:

Line 118: Why did authors show approximate value of the size of a PSL particle (~2 μm)? Please provide the exact sizes and type (Sample bottle has) of PSL particles given by Duke Scientific.

Responses and Revisions:

We have included this in the revised manuscript:
"During the measurement period, we used 1 μm and 2 μm fluorescent and non-fluorescent PSL microspheres (3K-990, B0100, 4K-02 and B0200, Duke Scientific, Inc.) for calibration."

Comments and suggestions:

Line 130: PM800 is confusing. We traditionally label the subscript of PM (particulate matter) based on the size cut in "micrometer". Please modify PM800 into PM0.8.

Responses and Revisions:

Corrected.

Comments and suggestions:

Figure 10: I feel this figure is meaningless because Tables 2, 3, and 4 covers what this figure illustrates.

Responses and Revisions:

Yes. We have deleted this figure in the revised manuscript.

Response to Anonymous Referee #2

We thank the reviewer for the constructive suggestions/comments. Below we provide a point-by-point response to individual comments (reviewer comments in italics, responses in plain font; page numbers refer to the ACPD version; figures used in the response are labeled as Fig. R1, Fig. R2,…).

Comments and suggestions:

To my experience, their fluorescent # concentration was too high for Nanjing. Based on previous UV-APS data, it was about 104/m3 in the summer (June-July time period). It was also observed that there were three fluorescent peaks (1, 2.5, and 3 um). Maybe the results were different because of different instrument and different time of the measurements. In Nanjing, probably fungal spore concentration levels are higher. If they can provide some culturable or PCR data, it would significantly improve their paper.

Responses and Revisions:

A previous study on bioaerosols in Nanjing (Wei et al., 2015) was performed by means of UV-APS (excitation at 355 nm and emission at 450-575 nm), which is similar to the FL3 channel of WIBS. Although Healy et al. (2014) found strong correlation (R^2=0.78) between FL3 channel and UV-APS, there was a systematic overestimation of the number concentration (~3 times), which is likely to be the different threshold selection method applied. In our study, the threshold for FL3 channel is set as 18 a.u., which is calculated based on equation (1). However, comparable number concentrations with clean environments (~0.1 cm^{-3}; Gabey et al., 2010; Huffman et al., 2012) and in the previous Nanjing study (~0.04 cm^{-3}; Wei et al., 2015) can be achieved by setting the threshold to 80-200 a.u. (FL3), as shown in Fig.R1. The impact of the applied threshold level might be more critical in polluted areas than the clean environments due to the higher fraction of anthropogenic emissions. Hence, the requirement of establishing standard calibration procedures is required in future studies. As mentioned by the referee, different sampling times might also introduce a bias in number concentrations. We have clarified this in the revised manuscript.

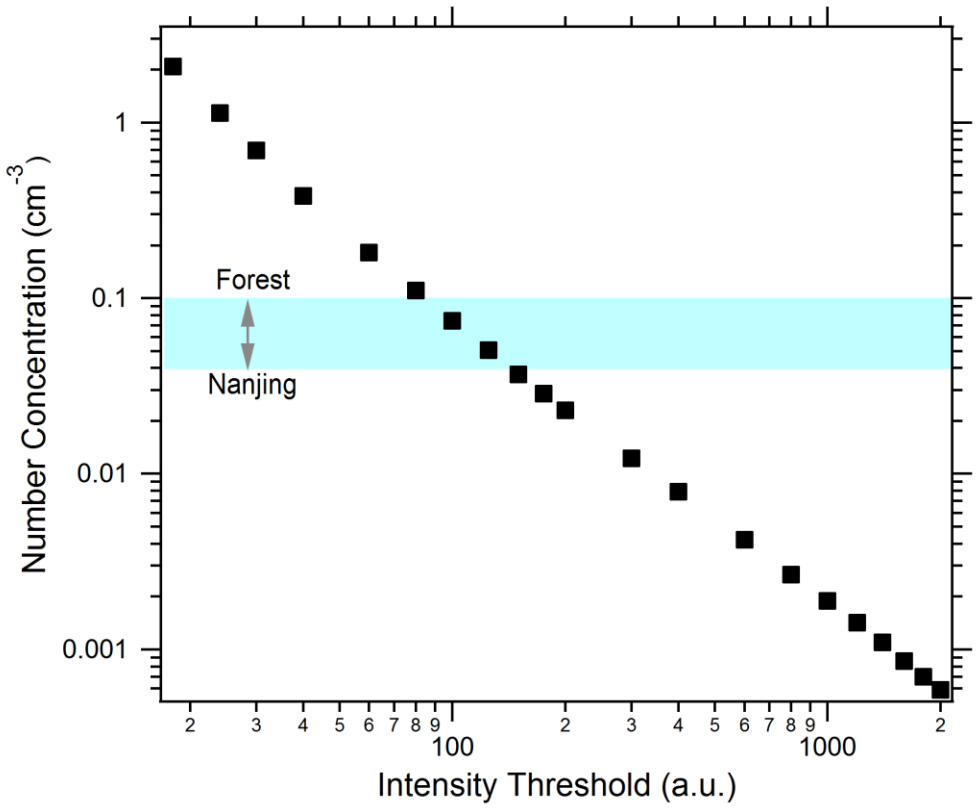

Figure R1. Average number concentrations of FAPs in FL3 channel using different threshold. The shaded area indicates the previous measured number concentrations in clean environments (~0.1 cm^{-3}; Gabey et al., 2010; Huffman et al., 2012) and in the previous Nanjing study (~0.04 cm^{-3}; Wei et al., 2015).

The SORPES station was influenced by the anthropogenic activities (Herrmann et al., 2014), indicating that local fluorescent aerosol particles may contain some non-biological fluorophores. We agree with the referee that comparison with culturable or PCR data would improve any WIBS data analysis and characterization of bio-aerosol, respectively. Unfortunately, this kind of information was not gathered during the campaign and cannot be retrieved in retrospect."

Comments and suggestions:

It was still not clear that how much percent of the measured fluorescent particles can be attributed to real microbial aerosol particles (e.g., bacteria and fungal spores). The authors mentioned that combustion generated aerosols might contribute to the fluorescent particles. Could the authors further expand the discussion about the types of combustions? e.g., agriculture burning, traffic, cooking, coal burning and etc. What was the major contributor?

Responses and Revisions:

In our study, we found that biological particles cannot be explicitly identified by WIBS, especially in the polluted environment. Therefore, we proposed two alternative data retrieval methods as proxy to distinguish bioaerosols. Two groups were classified as "non-combustion-related", tentatively bioaerosols type particles, accounting for ~15% and ~16% to the total fluorescent aerosol particles. Still, these two methods can't distinguish specific species. As a result of our study, and in agreement with the referee's suggestions, we propose to complement WIBS observations with other techniques, such as molecular techniques (PCR, sequencing methods, and so on) in future studies in highly polluted environments.

Figure R2 shows the particle number size distributions from different sources. Our measurements revealed a pattern in the coarse mode (D >1 μm) which is similar to biomass burning particles (Hungershoefer et al., 2008). Both of them are dominated by the particles in the size range of 1-2 μm, with the fractions of 90% and 80% of the total number concentrations, respectively. On the contrary, particles from diesel vehicle emissions (Morawska et al., 1998) showed a different distribution in the coarse mode, and the contribution of particles in the size range of 1-2 μm was only 37%. Pöhlker et al. (2012) reported that interferents like PAHs, can be particularly enriched on the surface of soot particles from biomass burning. Therefore a possible origin of these CR particles might be biomass burning.

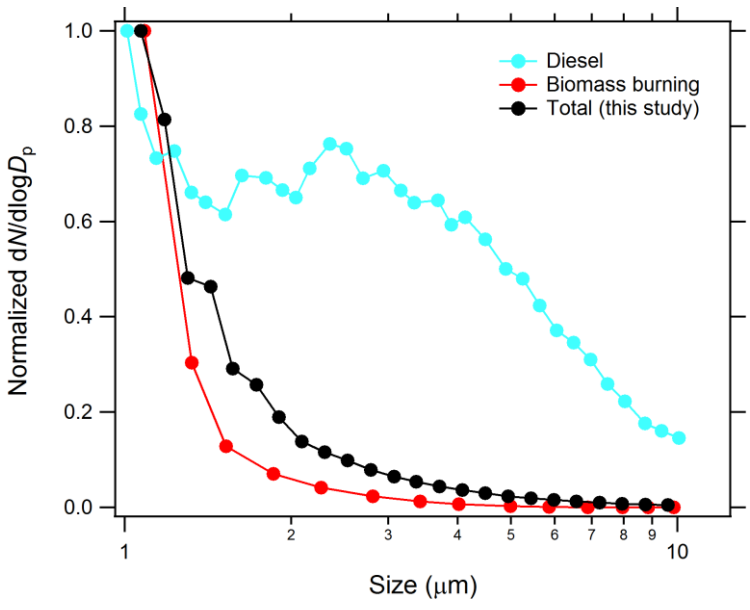

Figure R2. Comparisons of particle number size distributions from different sources.

Comments and suggestions:

Their results are based on one city measurement, and some results might be limited because of different climatic conditions, ecology settings and human activities.

Nonetheless, it seems the diurnal pattern was similar to those of other parts of China and the world because of the boundary layer effect. In future studies, it would be great to see the fluorescent particle diurnal pattern for those regions without boundary layer effect or at least minimal.

Responses and Revisions:

As referee mentioned, the effect of the boundary layer may result in the similar diurnal variation of different kinds of fluorescent particles. To minimize the impacts of transport and boundary layer, we also demonstrated the diurnal variation of fluorescent particles fraction, and the different diurnal pattern was found for various fluorescent aerosol particles, as shown in Fig. R3.

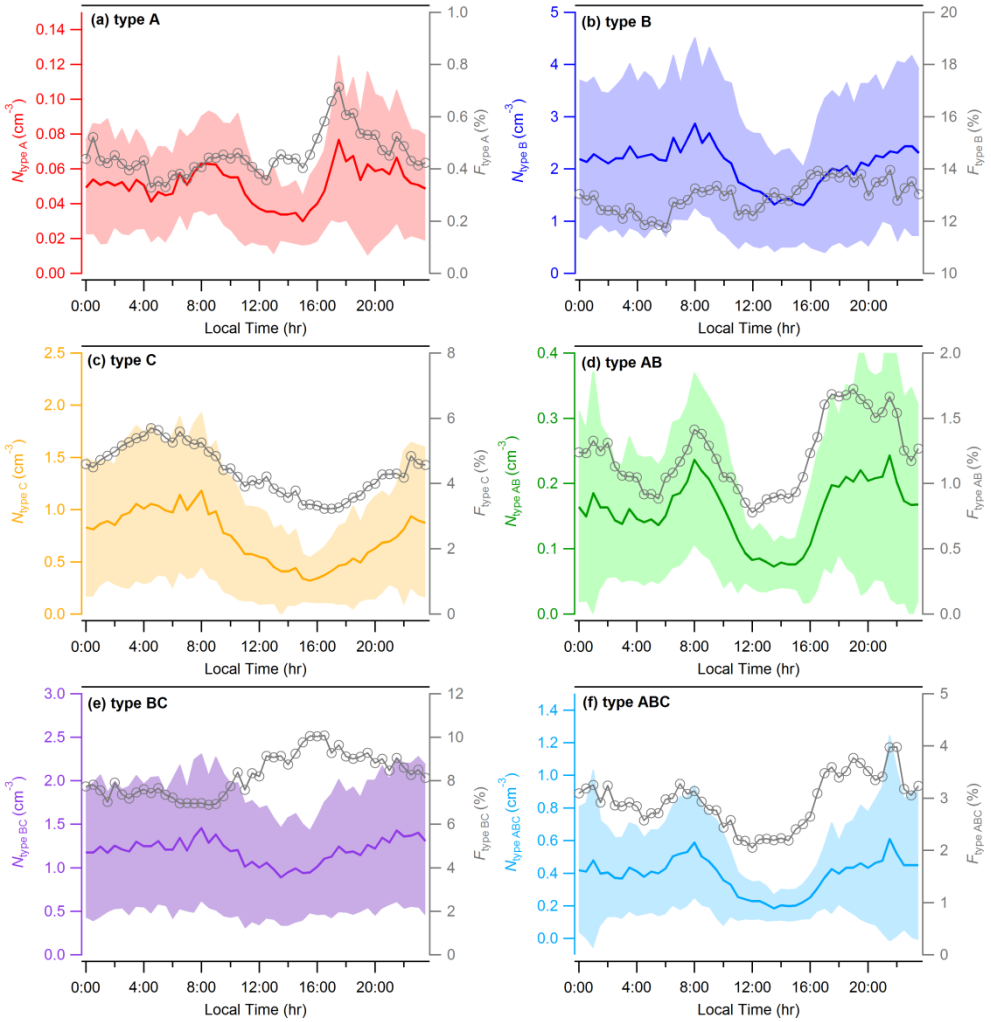

Figure R3. Diurnal variations of number concentrations of (a) type A, red, (b) type B, blue, (c) type C, dark yellow, (d) type AB, green, (e) type BC, purple and (f) type ABC, light blue. Gray line indicates the number fraction of respective total fluorescent particles (right axis). Shading indicates ± one standard deviation.

The following two approaches can be used to untangle the boundary layer effect: (1) using modelling tools to account for the boundary layer effect and investigate the concentration diurnal profile under different emission schemes; or (2) performing aircraft measurements (or other high altitude) above the boundary layers.

References

Gabey, A. M., Gallagher, M. W., Whitehead, J., Dorsey, J. R., Kaye, P. H., and Stanley, W. R.: Measurements and comparison of primary biological aerosol above and below a tropical forest canopy using a dual channel fluorescence spectrometer, Atmos Chem Phys, 10, 4453-4466, 10.5194/acp-10-4453-2010, 2010.

Healy, D. A., Huffman, J. A., O'Connor, D. J., Pöhlker, C., Pöschl, U., and Sodeau, J. R.: Ambient measurements of biological aerosol particles near Killarney, Ireland: a comparison between real-time fluorescence and microscopy techniques, Atmos. Chem. Phys., 14, 8055-8069, 10.5194/acp-14-8055-2014, 2014.

Herrmann, E., et al.: Aerosols and nucleation in eastern China: first insights from the new SORPES-NJU station, Atmos. Chem. Phys., 14, 2169-2183, 10.5194/acp-14-2169-2014, 2014.

Huffman, J. A., Sinha, B., Garland, R. M., Snee-Pollmann, A., Gunthe, S. S., Artaxo, P., Martin, S. T., Andreae, M. O., and Pöschl, U.: Size distributions and temporal variations of biological aerosol particles in the Amazon rainforest characterized by microscopy and real-time UV-APS fluorescence techniques during AMAZE-08, Atmos Chem Phys, 12, 11997-12019, 10.5194/acp-12-11997-2012, 2012.

Hungershoefer, K., et al.: Modelling the optical properties of fresh biomass burning aerosol produced in a smoke chamber: results from the EFEU campaign, Atmos. Chem. Phys., 8, 3427-3439, 10.5194/acp-8-3427-2008, 2008.

Morawska, L., Bofinger, N. D., Kocis, L., and Nwankwoala, A.: Submicrometer and Supermicrometer Particles from Diesel Vehicle Emissions, Environ Sci Technol, 32, 2033-2042, 10.1021/es970826+, 1998.

Pöhlker, C., Huffman, J. A., and Pöschl, U.: Autofluorescence of atmospheric bioaerosols – fluorescent biomolecules and potential interferences, Atmos. Meas. Tech., 5, 37-71, 10.5194/amt-5-37-2012, 2012.

Wei, K., Zheng, Y., Li, J., Shen, F., Zou, Z., Fan, H., Li, X., Wu, C.-y., and Yao, M.: Microbial aerosol characteristics in highly polluted and near-pristine environments featuring different climatic conditions, Science Bulletin, 60, 1439-1447, 10.1007/s11434-015-0868-y, 2015.

Ambient measurement of fluorescent aerosol particles with a WIBS in the Yangtze River Delta of China: potential impacts of combustion-related aerosol particles

X. Yu[1,2], Z. Wang[2], M. Zhang[2], U. Kuhn[2], Z. Xie[1], Y. Cheng[2], U. Pöschl[2], H. Su[2]

[1]School of Earth and Space Sciences, University of Science and Technology of China, Hefei 230026, China

[2]Multiphase Chemistry Department, Max Planck Institute for Chemistry, Mainz 55128, Germany

Correspondence to Zhibin Wang (Zhibin.Wang@mpic.de) and Zhouqing Xie (zqxie@ustc.edu.cn)

Abstract

Fluorescence characteristics of aerosol particles in polluted atmosphere were studied using a wideband integrated bioaerosol spectrometer (WIBS-4A) in Nanjing, Yangtze River Delta area of China. We observed strong diurnal and day-to-day variations of fluorescent aerosol particles (FAPs). The average number concentrations of FAPs (1-15 μm) detected in the three WIBS measurement channels (FL1: 0.6 cm^{-3}, FL2: 3.4 cm^{-3}, FL3: 2.1 cm^{-3}) were much higher than those observed in forests and rural areas, suggesting that FAPs other than bioaerosols were detected. We found that the number fractions of FAPs were positively correlated with the black carbon mass fraction, especially for the FL1 channel, indicating a large contribution of combustion-related aerosols. To distinguish bioaerosols from combustion-related FAPs, we investigated two classification schemes for use with WIBS data. Our analysis suggests a strong size dependence for the fractional contributions of different types of FAPs. In the FL3 channel, combustion-related particles seem to dominate the 1-2 μm size range while bioaerosols dominate 2-5 μm. The number fractions of combustion-related particles and non-combustion-related particles to total aerosol particles were ~11% and ~5%, respectively.

1 Introduction

From the beginning of atmospheric aerosols studies, airborne biological particles have been found as an important class of aerosol particles (Bary et al., 1887; Haldane and Anderson, 1887; Després et al., 2012). They are ubiquitous in the atmosphere with a wide size range from approximately several nanometers to a few hundred micrometers (Pöschl, 2005; Després et al., 2012). Primary biological aerosol particles (PBAPs) are a subset of biological particles, usually defined as the aerosols of biological origin or carry living organisms, including viruses, bacteria, fungal, pollen, cell or plant debris and animal tissue (Huffman et al., 2012). PBAPs can affect the Earth's radiation balance directly by absorbing and scattering solar radiation, and indirectly by serving as giant cloud condensation nuclei (CCN) and ice nuclei (IN), and thereby influence cloud microphysical and climate-relevant properties (Christner et al., 2008; Pöschl et al., 2010; Deleon-Rodriguez et al., 2013; Morris et al., 2013). These impacts are not only restricted to a local scale, but may also be effective in a regional scale due to the transport of bioaerosols, e.g., by dust storms (Griffin, 2007; Polymenakou et al., 2008; Hallar et al., 2011; Creamean et al., 2013). In addition, PBAPs can spread human, animal and plant disease and influence public health (Després et al., 2012; Cao et al., 2014). Considering its comprehensive impacts in diverse scientific fields, a better understanding of PBAPs such as its concentration, composition, spatial and temporal variability becomes critically important.

Despite its importance, information of PBAPs in the atmosphere is still very limited. Further investigation is hindered due to the lack of automatic measurement techniques. Most previous studies are based on the analysis of cultivable PBAPs or DNAs from filter samples (Henningson and Ahlberg, 1994; Duchaine et al., 2001; Yu et al., 2013). These methods are time-consuming and their results may differ depending on the cultivation condition and procedures, especially considering the ubiquity of microorganisms that cannot be cultivated (Oliver, 2005; Pöhlker et al., 2012). The low time resolution of cultivation methods makes it difficult to investigate the emission mechanisms of PBAPs, which happen at a time scale of less than a few hours.

Since most biological materials contain fluorophores, instruments based on the fluorescence detection, such as UV-APS (Ultraviolet Aerodynamic Particle Sizer) (Brosseau et al., 2000), WIBS (Wideband Integrated Bioaerosol Spectrometer) and other custom-made instruments based on the LIF (Laser induced fluorescence) technology (Pan et al., 2009; Taketani et al., 2013; Miyakawa et al., 2015), have recently been developed for online measurements of PBAPs. These instruments have been applied in various atmospheric environments, including rainforest (Gabey et al., 2010; Huffman et al., 2012), forest (Huffman et al., 2013; Schumacher et al., 2013; Crawford et al., 2014), high-altitude (Gabey et al., 2013; Valsan et al., 2016), rural (Healy et al., 2014), suburban (Huffman et al., 2010; Toprak and Schnaiter, 2013) and urban environments (Gabey et al., 2011; Miyakawa et al., 2015; Wei et al., 2016). Besides settled sampling sites, WIBS has also been used for airborne observations (Perring et al., 2015). In clean environments, these techniques can effectively distinguish PBAPs from other kinds of aerosol particles. For example, Huffman et al. (2012) found similar size distributions of PBAPs measured by UV-APS and scanning electron microscopy (SEM) in the Amazon rainforest.

PBAPs, however, are not the only fluorescent aerosol particles (FAPs) in the atmosphere. Other materials such as polycyclic aromatic hydrocarbons (PAHs) and humic-like substances (HULIS) may also fluoresce and contribute to the measured fluorescence signals (Pöhlker et al., 2012). Hence, the fluorescent information given by the instruments based on the fluorescence detection may include both fluorescent biological and non-biological particles.

In order to have a deeper insight into the ambient FAPs in polluted area, we have performed WIBS measurements in Nanjing, China in the autumn of 2013. In this study, we first present the number concentration of FAPs in Nanjing in comparison to previous studies. Then we demonstrate the potential impacts of combustion-related aerosol particles in discrimination of bioaerosols under the polluted atmosphere. Finally, we introduce alternative methods to quantify the relative contributions of different fluorescent materials (combustion- and bioaerosol-type particles) to FAPs.

2 Methods and instrumentation

2.1 Site description

WIBS measurements were performed at the Station for Observing Regional Processes of the Earth System (SORPES station), Xianlin campus of Nanjing University (32.12 °N, 118.95 °E). Nanjing lies in the Yangtze River Delta with a total population of 8.18 million (data of 2013), and it's a large commercial center in the East China region. The measurement site is ~20 km in the east of the urban center. The SORPES station is located on a hill about 40 m above the surroundings. Details of this station were described by Ding et al. (2013). A 0.75 inch stainless-steel tube inlet was installed ~3 m above the roof, and sample air was dried by a vertical silica gel drier prior to entering the WIBS. Data were collected from 29 October to 15 November 2013.

2.2 Instruments

Measurements of FAPs were performed with a WIBS-4A. It uses the single-particle elastic scattering intensity at 535 nm to calculate the optical size of particles. The scattering signal is used to trigger the flash of two xenon lamps with UV wavelength of 280 nm and 370 nm, respectively. The fluorescent signals are recorded at two wavelength bands (310-400 nm and 420-650 nm). This design results in three wavelength channels: FL1 with excitation at 280 nm and detection 310–400 nm, FL2 with excitation wavelength at 280 nm and detection wavelength at 420–650 nm, and FL3 with excitation wavelength at 370 nm and detection wavelength at 420-650 nm. Respective abbreviations are listed in Table 1. During the measurement period, we used 1 μm and 2 μm fluorescent and non-fluorescent PSL microspheres (3K-990, B0100, 4K-02 and B0200, Duke Scientific, Inc.) for calibration. The fluorescence noise threshold is defined as:

$$E_{\text{Threshold}} = E + 3\sigma \quad (1)$$

Where E is the modal baseline and σ is the standard deviations in each channel. Particles with fluorescence signals above the noise threshold are classified as FAPs. Single-particle data were converted into a size distribution with a 5-min integration time and particles with diameter of 1-15 μm were analyzed in this study.

Meteorological data were collected with an Automatic Weather Station (CAMPBEL co., AG1000). The differential mobility particle sizer (DMPS, built at Helsinki University)

was used to measure the number size distribution of sub-micron particles between 6 and 800 nm mobility diameter (Herrmann et al., 2014). Particle mass concentration below 0.8 μm ($PM_{0.8}$) was calculated from the measured size distributions assuming a density of 1.6 g cm^{-3} (Wang et al., 2014). A 7-wavelength "Spectrum" Aethalometer (AE-31, Magee Scientific co.) was used to measure the black carbon (BC) mass concentration $M_{BC.}$

3 Results and discussion

3.1 Non-biological fluorescent aerosol particles

Figure 1 shows the time series of number concentrations and fractions of FAPs during the measurement period. The number concentration of FAPs was dominated by FL2 channel with a mean number concentration N_{FL2} of 3.4 cm^{-3}, followed by N_{FL3} of 2.1 cm^{-3} and N_{FL1} of 0.6 cm^{-3}. These number concentrations were 1~2 order of magnitudes higher than those observed in clean areas where bioaerosols dominate the FAPs (Table 2). For example, FAPs of 0.093 cm^{-3}, 0.15 cm^{-3} and 0.023 cm^{-3} were reported for the Amazon, Borneo and Hyytiälä forests, respectively (Gabey et al., 2010; Huffman et al., 2012; Toprak and Schnaiter, 2013). Since polluted areas are characterized by less plants and natural biological processes, less bioaerosols are expected compared to the forests. This much higher number concentration of FAPs observed in Nanjing suggests other kinds of FAPs being detected by WIBS.

Previous studies (Pöhlker et al., 2012; Miyakawa et al., 2015; Perring et al., 2015) reported that non-biological compounds like PAHs, mineral dust and HULIS can also fluoresce. Several non-biological fluorophores such as SOAs, pyrene, humic acid and naphthalene have fluorescent property in the same excitation and emission wavelength bands of FL1 channel (Chang and Thompson, 2010; Pöhlker et al., 2012). These materials originate from sources different from bioaerosols. For example, PAH enriches on the surface of soot particles from biomass burning and fuel combustion, challenging the interpretation of ambient particle fluorescence measurements.

Our sampling site is located in the vicinity of the polluted Nanjing city and is intensively affected by human activities. To check the potential influences of PAH and combustion processes, we compared the variability of FAPs with that of BC, on which the PAHs are often coated. To minimize the impacts of transport and boundary layer

dynamics, we compared the ratio of BC and FAPs to the total particles in their respective size range, i.e., $M_{BC}/PM_{0.8}$ and F_x instead of using absolute concentrations. Miyakawa et al. (2015) used factor analysis based on carbon monoxide, elemental carbon and other markers (using concentration instead of ratio) to identify "combustion-type" and "dust-type" aerosols in urban areas. In our study, we found that $M_{BC}/PM_{0.8}$ showed a good correlation with the number fraction of FAPs, especially in the FL1 channel (r=0.748, Fig.1). For FL2 and FL3 channels, the number fractions also nicely followed the variation of $M_{BC}/PM_{0.8}$ except for November 8, which deteriorated the overall correlation. Since BC and PAHs are products of incomplete combustion, the similar variability suggests a large contribution from combustion-related aerosols to the measured FAPs, especially in FL1 channel. Our findings strongly support previous results (Toprak and Schnaiter, 2013; Miyakawa et al., 2015) that FAPs (FL1 channel) may came from combustion process and anthropogenic interference.

3.2 Spectral patterns of fluorescent aerosol particles

The complex nature of FAPs in polluted areas challenges the interpretation of ambient measurements. Different fluorophores have their characteristic excitation-emission matrices (EEM) map, which can be useful for discrimination of biological from non-biological FAPs (Pöhlker et al., 2012). Since WIBS only has two excitation and emission wavebands, a high-resolution EEM map cannot be retrieved. But we can still consider the two wavebands as a low resolution EEMs, of which the distribution (i.e., the ratio of the two wavebands) may also contain information about the nature of FAPs. For example, we can assume two kinds of fluorescent compounds I and II have different fluorescent spectra, as shown in Fig. 2a. For each compound, the integrated fluorescence intensity are determined in two wavebands by WIBS (Fig. 2b). For qualitative analysis, a normalized EEM is often used providing the relative wavelength dependence of fluorescent materials. For WIBS, we simply used the ratio of fluorescence intensity from different WIBS channels to represent the wavelength dependence (Fig. 2c).

Figure 3 shows the intensity distributions of aerosols particles in different fluorescence bands/channels. Due to the instrument setting, fluorescence signal intensities beyond 2200 arbitrary units (a.u.) are forced to the range of 2000-2200 a.u., regarding as saturated signal. Hence we only discussed fluorescence signal intensities

below 2000 a.u.. We first investigated the intensity ratio between channel FL1 and FL2, as shown in Fig. 3a. With increasing fluorescence intensity, the number concentrations sharply dropped, i.e., most of the abundant aerosol particles exhibited no or only weak fluorescence. Using the intensity ratio of FL1 to FL2 (I_{FL1}/I_{FL2}) as a fluorescence fingerprint, we obtained two prominent groups of aerosols with I_{FL1}/I_{FL2} approaching 0 or infinity. $I_{FL1}/I_{FL2} \sim 0$ means that the aerosol have a low FL1 intensity below the detection limit and a high FL2 intensity, while I_{FL1}/I_{FL2} approaching infinity means the opposite. According to the detection thresholds of both FL1 and FL2 channels, we then classified the aerosol particles into four groups with FL1/FL2 above or below the detection threshold (labelled as g1 to g4 in Fig. 3). We further investigated the FL3 properties of the various groups. As shown in Figs. 3b-3d, the aerosol number concentration decreased as FL3 intensity increased resembling the distribution for FL1 and FL2. Similarly we used the fluorescence threshold of FL3 to classify aerosols from g1 to g4 into subgroups.

Our efforts towards a spectral fingerprint resulted in the same classification method as in Perring et al. (2015). Here we adopted the labels of Perring et al. (2015) in which channel A refers to FL1, channel B refers to FL2 and channel C refers to FL3. Any aerosol particle can have signals above/below the fluorescence threshold in any of these channels, leading to seven combinations of fluorescence signals, i.e., particles with fluorescence signals above the threshold in single channel as types A, B and C; particles with fluorescence signals in two channels as types AB, AC and BC and particles with fluorescence signals in all three channels as type ABC (Table 1).

As shown in Fig.4a, types B, BC and C were the most abundant FAPs, followed by types ABC, AB and A. Type AC had the lowest loading and was not even visible. The mean number concentrations of dominant types B, BC and C were 1.77 cm^{-3}, 1.06 cm^{-3} and 0.66 cm^{-3}, respectively (Table 3). The number concentration of 7-type FAPs exhibited strong diurnal and day-to-day variability (Fig. 5). Number concentration of FAPs peaked in the morning (~08:00 local time) and reached a minimum in the afternoon (~14:00). Their similar diurnal patterns indicate the dominant effect of boundary layer development in controlling the variability of aerosol particles, which was also shown in FL1, FL2 and FL3 channels (Figure S1). To better understand the source of FAPs, we also investigated the number fraction of FAPs in total particles. The boundary layer

development exerts similar effect on all kinds of aerosol particles. Thus for particles of the same origin, their ratios will remain constant and a difference in their ratios reflects their different sources. As shown in Fig. 5, the fractions of FAPs presented quite different diurnal patterns. The fractions of type BC revealed substantial diurnal opposite with a clear morning peak and early afternoon minimum. Type A and type B showed a much weaker variability, implying a similar source of FAPs as the total aerosol particles.

The number size distributions of FAPs were shown in Figure 6. The highest FAPs number concentration came out at ~1 μm except type ABC. Type ABC peaked at 1-2 μm with a second peak at 4-6 μm. For type A, type C and type BC the number concentration monotonously decreased with size increased. No fluorescence signals were found in FL1 and FL3 channels (corresponding to type A, type C and type AC FAPs) for the particles of size larger than 4 μm. On the contrary, the number fractions of FAPs generally increased as the particle size increased, reaching ~100% at 3-4 μm for FL2 channel (not shown in Fig.6). These results reveal that most coarse mode particles contain certain kinds of fluorophores.

Meanwhile, we compared the number fraction of 7-type FAPs with $M_{BC}/PM_{0.8}$, the results indicate that the number fractions of types A, AB, and ABC showed good correlations with $M_{BC}/PM_{0.8}$ (Fig. 7), suggesting a large contribution of combustion-related aerosol particles to these types. Note that all these types contain FL1 signals, implying the potential application of FL1 in the identification of biomass burning (or other combustions) events. Likewise, fluorescent types B and BC mostly followed the variation of $M_{BC}/PM_{0.8}$ except for November 8 when elevated fractional contributions were observed one day before a rain event on November 9. A dramatic release of certain fungal spores was often observed before rain (Hjelmroos, 1993). However, the increase on November 8 was mainly contributed by 1-2 μm FAPs rather than fungal spores (> 3 μm) shown by Hjelmroos (1993). So the origin of this elevated FAPs remained inconclusive. Moreover, good correlation (r=0.58) between type B particles in 3-4 μm and $M_{BC}/PM_{0.8}$, suggesting a closer link of this peak with type B particles to combustion process. Fluorescent type C showed a weak negative correlation with $M_{BC}/PM_{0.8}$, suggesting a minor role of combustion-related aerosols or major contribution of non-combustion related aerosols (e.g., bioaerosols or dusts).

3.3 Fluorescence intensity

Besides the relative wavelength dependence, the absolute quantum yield is also one of the most important characteristics of a fluorophore. Discrepancies in the quantum yield can directly influence the fluorescence, resulting in different intensity levels. Thus it is possible to use the intensity information to identify different kinds of FAPs. Huffman et al. (2012) showed that the UV-APS can be used to successfully discriminate bioaerosols from dust particles, both of which have been suggested to fluoresce (Pöhlker et al., 2012).

We first made a hypothesis that there exists a characteristic intensity value I_{cri}, above which most FAPs are bioaerosols. Since I_{cri} cannot be directly inferred from the intensity distribution (Fig. 3), we adopted the parameter $M_{BC}/PM_{0.8}$ to assist our analysis. This is because bioaerosols and combustion-related FAPs are of different origins, we scanned different values for I_{cri} until the corresponding FAPs (of intensity> I_{cri}) fraction showed a non-positive correlation with $M_{BC}/PM_{0.8}$. In this study, we mainly focus on the FL3 channel since it is running in a similar excitation-emission wavelength as the UV-APS and it has been validated against other independent method. We thereby suggest that FL3 channel can be used to discriminate bioaerosols from combustion-generated FAPs in a similar approach. The analysis of FL1 and FL2 channels were shown in the supplementary Information (Figure S2 and Figure S3). Figure 8 shows the averaged fractional contribution of FAPs with $I_{FL3}>I_{cri}$ at different $M_{BC}/PM_{0.8}$ levels. To account for the size dependence of fluorescence signals, we first classified FAPs according to the particle size. For the 1-2 μm size range, the fraction was always positively correlated with $M_{BC}/PM_{0.8}$ and was independent of the selection of I_{cri}. For the size range of 2-5 μm, the FAPs showed mostly negative correlation with $M_{BC}/PM_{0.8}$ and were also independent of the I_{cri} selection. For FAPs larger than 5 μm, the selection of I_{cri} became critical. With increasing I_{cri}, the dependence of FL3 fraction on $M_{BC}/PM_{0.8}$ gradually became weaker and finally turned to negative at I_{cri} > 40 a.u.. The results at 5-15 μm were consistent with our hypothesis that bioaerosols have stronger fluorescence intensity than combustion-related aerosol particles and can be discriminated from their fluorescence intensity. The different correlation statistics of 1-2 μm and 2-5 μm may be explained by the different abundance of bioaerosols and combustion-related aerosols at different size range. The 2-5 μm mode was dominated by bioaerosols, while the 1-2 μm mode was dominated by

combustion-related aerosol particles. Therefore there was no clear dependence on the selection of I_{cri}. Saari et al. (2015) reported that FAPs at 0.5-1.5 μm might be due to anthropogenic emissions such as biomass burning, while most fungal spores and pollen dominated the larger size range (Després et al., 2012). It is also possible that I_{cri} had a size dependence because different types of bioaerosols may dominate different size ranges.

By integrating the FAPs of different correlations with $M_{BC}/PM_{0.8}$, we retrieved the number concentrations of "non-combustion-related" (NCR) type particles (FAPs with I_{FL3}>18 a.u. at 2-5 μm and FAPs with I_{FL3}>40 a.u. at 5-15 μm) and "combustion-related" (CR) type particles (FAPs with I_{FL3}>18 a.u. at 1-2 μm and FAPs with 40≥I_{FL3}>18 a.u. at 5-15 μm). The mean number concentrations of NCR type and CR type particles were 0.64±0.46 cm^{-3} and 1.45±1.06 cm^{-3}, respectively. The NCR type FAPs are likely bioaerosols.

In this study, we applied two methods to classify FAPs measured by WIBS, resulting in two non-combustion-types of particles: type C particles derived from fluorescent spectral pattern analysis and NCR type particles derived from fluorescence intensity pattern analysis. As shown in Table 3, the mean number concentrations of type C and NCR type particle were 0.66 cm^{-3} and 0.64 cm^{-3}, which were still higher than those found in PBAPs-dominated regions like the Amazon (Huffman et al., 2012), Hyytiälä (Schumacher et al., 2013) and PdD (Gabey et al., 2013). This indicates that still a residual of these non-combustion type particles may comprise other fluorescent constituents like mineral dusts (Miyakawa et al., 2015; Perring et al., 2015).

4. Conclusions

On-line measurements of FAPs have been performed in Nanjing by using WIBS in the autumn of 2013. Our results showed that the number concentrations of FAPs were 1~2 order of magnitudes higher than those reported in the previous studies. The observed high values suggested that directly using FL1, FL2 and FL3 channels to index PBAPs is not suitable for polluted areas. The number fraction of FL1 showed strong correlation with $M_{BC}/PM_{0.8}$ (r=0.748), indicative of a strong bias by anthropogenic emissions.

In this study, we used two methods to classify the FAPs. According to the threshold of each channel, FAPs were divided into 7 types. Number fraction of type C showed negative correlation (r=-0.13) with $M_{BC}/PM_{0.8}$, which might be more representative for bioaerosols. Meanwhile, on the basis of the FL3 fluorescent intensity and its correlations with $M_{BC}/PM_{0.8}$, FL3 fluorescent particles were divided into 2 types. Combustion-related type particles seemed to dominate 1-2 μm, while the non-combustion-related type particles, which concentrated in the size range of 2-5 μm and showed negative correlation (r=-0.121) with $M_{BC}/PM_{0.8}$, might be originated from biological emissions. The number concentrations of the identified two types of bioaerosols (0.66 cm^{-3} for type C particles and 0.64 cm^{-3} for non-combustion-related type), however, were still higher than those observed in clean background areas and previous study in Nanjing (Wei et al., 2015), indicating they may also include some other fluorophores, such as dusts.

Our results suggested that fluorescence measurements in polluted areas are prone to interferences and uncertainty introduced by the anthropogenic emissions. Discrimination of biological particles from FAPs still needs further development. Each fluorophore species presents unique fluorescence spectrum, hence we can effectively distinguish biological particles from other FAPs based on their specific EEM maps. Due to the limitation of excitation and emission wavebands of WIBS, the development of a multi-wavebands instrument is hence needed. Other methods such as the cluster analysis (Robinson et al., 2013; Crawford et al., 2014; Crawford et al., 2015) also exhibited the ability to differentiate various FAPs. Measuring additional particle properties such as size and morphology will help ameliorate the interferences by providing additional dimensions to distinguish fluorescent particles of different emission mechanisms.

Acknowledgments

This study was supported by the Max Plank Society (MPG), the European Commission under the projects BACCHUS (Grant No. 603445) and the Natural Science Foundation of China (Project No. 91544103). Xiawei Yu and Minghui Zhang would like to thank the China Scholarship Council (CSC) for financial support. We thank the SORPES-NJU station for logistic and instrumentation support.

References

Bary, A., Garnsey, H. E. F., and Balfour, I. B.: Comparative morphology and biology of the fungi, mycetozoa and bacteria, Clarendon Press, 1887.

Brosseau, L. M., Vesley, D., Rice, N., Goodell, K., Nellis, M., and Hairston, P.: Differences in Detected Fluorescence Among Several Bacterial Species Measured with a Direct-Reading Particle Sizer and Fluorescence Detector, Aerosol Sci. Technol., 32, 545-558, 10.1080/027868200303461, 2000.

Cao, C., Jiang, W., Wang, B., Fang, J., Lang, J., Tian, G., Jiang, J., and Zhu, T. F.: Inhalable Microorganisms in Beijing's PM2.5 and PM10 Pollutants during a Severe Smog Event, Environ Sci Technol, 48, 1499-1507, 10.1021/es4048472, 2014.

Chang, J. L., and Thompson, J. E.: Characterization of colored products formed during irradiation of aqueous solutions containing H 2 O 2 and phenolic compounds, Atmos. Environ., 44, 541-551, 2010.

Christner, B. C., Morris, C. E., Foreman, C. M., Cai, R., and Sands, D. C.: Ubiquity of Biological Ice Nucleators in Snowfall, Science, 319, 1214, 10.1126/science.1149757, 2008.

Crawford, I., Robinson, N. H., Flynn, M. J., Foot, V. E., Gallagher, M. W., Huffman, J. A., Stanley, W. R., and Kaye, P. H.: Characterisation of bioaerosol emissions from a Colorado pine forest: results from the BEACHON-RoMBAS experiment, Atmos Chem Phys, 14, 8559-8578, 10.5194/acp-14-8559-2014, 2014.

Crawford, I., Ruske, S., Topping, D. O., and Gallagher, M. W.: Evaluation of hierarchical agglomerative cluster analysis methods for discrimination of primary biological aerosol, Atmos. Meas. Tech., 8, 4979-4991, 10.5194/amt-8-4979-2015, 2015.

Creamean, J. M., Suski, K. J., Rosenfeld, D., Cazorla, A., DeMott, P. J., Sullivan, R. C., White, A. B., Ralph, F. M., Minnis, P., Comstock, J. M., Tomlinson, J. M., and Prather, K. A.: Dust and Biological Aerosols from the Sahara and Asia Influence Precipitation in the Western U.S, Science, 339, 1572-1578, 10.1126/science.1227279, 2013.

DeLeon-Rodriguez, N., Lathem, T. L., Rodriguez-R, L. M., Barazesh, J. M., Anderson, B. E., Beyersdorf, A. J., Ziemba, L. D., Bergin, M., Nenes, A., and Konstantinidis, K. T.: Microbiome of the upper troposphere: Species composition and prevalence, effects of tropical storms, and atmospheric implications, P Natl Acad Sci USA, 10.1073/pnas.1212089110, 2013.

Després, V. R., Huffman, J. A., Burrows, S. M., Hoose, C., Safatov, A. S., Buryak, G., Fröhlich-Nowoisky, J., Elbert, W., Andreae, M. O., Pöschl, U., and Jaenicke, R.: Primary biological aerosol particles in the atmosphere: a review, Tellus B, 64, 2012.

Ding, A. J., Fu, C. B., Yang, X. Q., Sun, J. N., Zheng, L. F., Xie, Y. N., Herrmann, E., Nie, W., Petäjä, T., Kerminen, V. M., and Kulmala, M.: Ozone and fine particle in the western Yangtze River Delta: an overview of 1 yr data at the SORPES station, Atmos Chem Phys, 13, 5813-5830, 10.5194/acp-13-5813-2013, 2013.

Duchaine, C., Thorne, P. S., Mériaux, A., Grimard, Y., Whitten, P., and Cormier, Y.: Comparison of endotoxin exposure assessment by bioaerosol impinger and filter-sampling methods, Appl. Environ. Microbiol., 67, 2775-2780, 2001.

Gabey, A. M., Gallagher, M. W., Whitehead, J., Dorsey, J. R., Kaye, P. H., and Stanley, W. R.: Measurements and comparison of primary biological aerosol above and below a tropical forest canopy using a dual channel fluorescence spectrometer, Atmos Chem Phys, 10, 4453-4466, 10.5194/acp-10-4453-2010, 2010.

Gabey, A. M., Stanley, W. R., Gallagher, M. W., and Kaye, P. H.: The fluorescence properties of aerosol larger than 0.8 μm in urban and tropical rainforest locations, Atmos Chem Phys, 11, 5491-5504, 10.5194/acp-11-5491-2011, 2011.

Gabey, A. M., Vaitilingom, M., Freney, E., Boulon, J., Sellegri, K., Gallagher, M. W., Crawford, I. P., Robinson, N. H., Stanley, W. R., and Kaye, P. H.: Observations of fluorescent and

biological aerosol at a high-altitude site in central France, Atmos Chem Phys, 13, 7415-7428, 10.5194/acp-13-7415-2013, 2013.
Griffin, D. W.: Atmospheric movement of microorganisms in clouds of desert dust and implications for human health, Clin. Microbiol. Rev., 20, 459-477, Doi 10.1128/Cmr.00039-06, 2007.
Haldane, J., and Anderson, A.: The carbonic acid, organic matter, and micro-organisms in air, more especially of dwellings and schools, Philosophical Transactions of the Royal Society of London. B, 61-111, 1887.
Hallar, A. G., Chirokova, G., McCubbin, I., Painter, T. H., Wiedinmyer, C., and Dodson, C.: Atmospheric bioaerosols transported via dust storms in the western United States, Geophys. Res. Lett., 38, L17801, 10.1029/2011GL048166, 2011.
Healy, D. A., Huffman, J. A., O'Connor, D. J., Pöhlker, C., Pöschl, U., and Sodeau, J. R.: Ambient measurements of biological aerosol particles near Killarney, Ireland: a comparison between real-time fluorescence and microscopy techniques, Atmos Chem Phys, 14, 8055-8069, 10.5194/acp-14-8055-2014, 2014.
Henningson, E. W., and Ahlberg, M. S.: Evaluation of microbiological aerosol samplers: a review, J. Aerosol Sci., 25, 1459-1492, 1994.
Herrmann, E., Ding, A. J., Kerminen, V. M., Petäjä, T., Yang, X. Q., Sun, J. N., Qi, X. M., Manninen, H., Hakala, J., Nieminen, T., Aalto, P. P., Kulmala, M., and Fu, C. B.: Aerosols and nucleation in eastern China: first insights from the new SORPES-NJU station, Atmos Chem Phys, 14, 2169-2183, 10.5194/acp-14-2169-2014, 2014.
Hjelmroos, M.: Relationship between airborne fungal spore presence and weather variables: Cladosporium and Alternaria, Grana, 32, 40-47, 1993.
Huffman, J. A., Treutlein, B., and Pöschl, U.: Fluorescent biological aerosol particle concentrations and size distributions measured with an Ultraviolet Aerodynamic Particle Sizer (UV-APS) in Central Europe, Atmos Chem Phys, 10, 3215-3233, 10.5194/acp-10-3215-2010, 2010.
Huffman, J. A., Sinha, B., Garland, R. M., Snee-Pollmann, A., Gunthe, S. S., Artaxo, P., Martin, S. T., Andreae, M. O., and Pöschl, U.: Size distributions and temporal variations of biological aerosol particles in the Amazon rainforest characterized by microscopy and real-time UV-APS fluorescence techniques during AMAZE-08, Atmos Chem Phys, 12, 11997-12019, 10.5194/acp-12-11997-2012, 2012.
Huffman, J. A., Prenni, A. J., DeMott, P. J., Pöhlker, C., Mason, R. H., Robinson, N. H., Fröhlich-Nowoisky, J., Tobo, Y., Després, V. R., Garcia, E., Gochis, D. J., Harris, E., Müller-Germann, I., Ruzene, C., Schmer, B., Sinha, B., Day, D. A., Andreae, M. O., Jimenez, J. L., Gallagher, M., Kreidenweis, S. M., Bertram, A. K., and Pöschl, U.: High concentrations of biological aerosol particles and ice nuclei during and after rain, Atmos Chem Phys, 13, 6151-6164, 10.5194/acp-13-6151-2013, 2013.
Miyakawa, T., Kanaya, Y., Taketani, F., Tabaru, M., Sugimoto, N., Ozawa, Y., and Takegawa, N.: Ground-based measurement of fluorescent aerosol particles in Tokyo in the spring of 2013: Potential impacts of nonbiological materials on autofluorescence measurements of airborne particles, J. Geophys. Res. Atmos., 120, 1171-1185, 10.1002/2014jd022189, 2015.
Morris, C. E., Sands, D. C., Glaux, C., Samsatly, J., Asaad, S., Moukahel, A. R., Gonçalves, F. L. T., and Bigg, E. K.: Urediospores of rust fungi are ice nucleation active at > −10 °C and harbor ice nucleation active bacteria, Atmos Chem Phys, 13, 4223-4233, 10.5194/acp-13-4223-2013, 2013.
Oliver, J. D.: The viable but nonculturable state in bacteria, J Microbiol, 43, 93-100, 2005.
Pan, Y.-L., Pinnick, R. G., Hill, S. C., and Chang, R. K.: Particle-Fluorescence Spectrometer for Real-Time Single-Particle Measurements of Atmospheric Organic Carbon and Biological Aerosol, Environ. Sci. Technol., 43, 429-434, 10.1021/es801544y, 2009.

Perring, A. E., Schwarz, J. P., Baumgardner, D., Hernandez, M. T., Spracklen, D. V., Heald, C. L., Gao, R. S., Kok, G., McMeeking, G. R., McQuaid, J. B., and Fahey, D. W.: Airborne observations of regional variation in fluorescent aerosol across the United States, J Geophys Res-Atmos, 120, 1153-1170, 10.1002/2014JD022495, 2015.
Pöhlker, C., Huffman, J. A., and Pöschl, U.: Autofluorescence of atmospheric bioaerosols – fluorescent biomolecules and potential interferences, Atmos. Meas. Tech., 5, 37-71, 10.5194/amt-5-37-2012, 2012.
Polymenakou, P. N., Mandalakis, M., Stephanou, E. G., and Tselepides, A.: Particle size distribution of airborne microorganisms and pathogens during an intense African dust event in the eastern Mediterranean, Environ. Health Perspect., 116, 292-296, Doi 10.1289/Ehp.10684, 2008.
Pöschl, U.: Atmospheric aerosols: Composition, transformation, climate and health effects, Angewandte Chemie-International Edition, 44, 7520-7540, DOI 10.1002/anie.200501122, 2005.
Pöschl, U., Martin, S. T., Sinha, B., Chen, Q., Gunthe, S. S., Huffman, J. A., Borrmann, S., Farmer, D. K., Garland, R. M., Helas, G., Jimenez, J. L., King, S. M., Manzi, A., Mikhailov, E., Pauliquevis, T., Petters, M. D., Prenni, A. J., Roldin, P., Rose, D., Schneider, J., Su, H., Zorn, S. R., Artaxo, P., and Andreae, M. O.: Rainforest Aerosols as Biogenic Nuclei of Clouds and Precipitation in the Amazon, Science, 329, 1513-1516, 10.1126/science.1191056, 2010.
Robinson, N. H., Allan, J. D., Huffman, J. A., Kaye, P. H., Foot, V. E., and Gallagher, M.: Cluster analysis of WIBS single-particle bioaerosol data, Atmos. Meas. Tech., 6, 337-347, 10.5194/amt-6-337-2013, 2013.
Saari, S., Niemi, J., Rönkkö, T., Kuuluvainen, H., Järvinen, A., Pirjola, L., Aurela, M., Hillamo, R., and Keskinen, J.: Seasonal and Diurnal Variations of Fluorescent Bioaerosol Concentration and Size Distribution in the Urban Environment, Aerosol and Air Quality Research, 15, 572-581, 2015.
Schumacher, C. J., Pöhlker, C., Aalto, P., Hiltunen, V., Petäjä, T., Kulmala, M., Pöschl, U., and Huffman, J. A.: Seasonal cycles of fluorescent biological aerosol particles in boreal and semi-arid forests of Finland and Colorado, Atmos Chem Phys, 13, 11987-12001, 10.5194/acp-13-11987-2013, 2013.
Taketani, F., Kanaya, Y., Nakamura, T., Koizumi, K., Moteki, N., and Takegawa, N.: Measurement of fluorescence spectra from atmospheric single submicron particle using laser-induced fluorescence technique, J. Aerosol Sci., 58, 1-8, http://dx.doi.org/10.1016/j.jaerosci.2012.12.002, 2013.
Toprak, E., and Schnaiter, M.: Fluorescent biological aerosol particles measured with the Waveband Integrated Bioaerosol Sensor WIBS-4: laboratory tests combined with a one year field study, Atmos Chem Phys, 13, 225-243, 10.5194/acp-13-225-2013, 2013.
Valsan, A. E., Ravikrishna, R., Biju, C. V., Pöhlker, C., Després, V. R., Huffman, J. A., Pöschl, U., and Gunthe, S. S.: Fluorescent Biological Aerosol Particle Measurements at a Tropical High Altitude Site in Southern India during Southwest Monsoon Season, Atmos. Chem. Phys. Discuss., 2016, 1-80, 10.5194/acp-2016-265, 2016.
Wang, H., Zhu, B., Shen, L., Liu, X., Zhang, Z., and Yang, Y.: Size distributions of aerosol during the Spring Festival in Nanjing, Huan jing ke xue (in Chinese), 35, 442-450, 2014.
Wei, K., Zheng, Y., Li, J., Shen, F., Zou, Z., Fan, H., Li, X., Wu, C.-y., and Yao, M.: Microbial aerosol characteristics in highly polluted and near-pristine environments featuring different climatic conditions, Science Bulletin, 60, 1439-1447, 10.1007/s11434-015-0868-y, 2015.
Wei, K., Zou, Z., Zheng, Y., Li, J., Shen, F., Wu, C.-y., Wu, Y., Hu, M., and Yao, M.: Ambient bioaerosol particle dynamics observed during haze and sunny days in Beijing, Sci. Total Environ., 550, 751-759, http://dx.doi.org/10.1016/j.scitotenv.2016.01.137, 2016.
Yu, J., Hu, Q., Xie, Z., Kang, H., Li, M., Li, Z., and Ye, P.: Concentration and Size Distribution of Fungi Aerosol over Oceans along a Cruise Path during the Fourth Chinese Arctic Research Expedition, Atmosphere, 4, 337-348, 2013.

479

480

Tables

Table 1. Definition of abbreviations used in the text.

Short name	Description
PBAPs	Primary biological aerosol particles
FAPs	Fluorescent aerosol particles
FL1	Fluorescent detected in channel F1 280 (excitation at 280 nm, detection 310–400 nm)
FL2	Fluorescent detected in channel F2 280 (excitation at 280 nm, detection 420–650 nm)
FL3	Fluorescent detected in channel F2 370 (excitation at 370 nm, detection 420–650 nm)
Type A	Fluorescent particle signal in channel FL1 only
Type B	Fluorescent particle signal in channel FL2 only
Type C	Fluorescent particle signal in channel FL3 only
Type AB	Fluorescent particle signal in channels FL1 and FL2
Type AC	Fluorescent particle signal in channels FL1 and FL3
Type BC	Fluorescent particle signal in channels FL2 and FL3
Type ABC	Fluorescent particle signal in channels FL1, FL2 and FL3
N_x	Number concentration of each type particles
F_x	Number fraction of each type particles
M_{BC}	Mass concentration of black carbon
$PM_{0.8}$	Mass concentration of particles in the size range of 0.006-0.8 μm
D_o	Particle optical equivalent diameter
a.u.	Arbitrary units

Table 2. Comparisons between the results of this study and previous studies. Unit for the number concentration of fluorescent particles is L^{-1}. Numbers in brackets are the number fractions of fluorescent particles (%).

Site Location	Site Category	Season	N_{FL1}	N_{FL2}	N_{FL3}	N_{FAPs}	References
Nanjing, China	sub-urban	autumn	570 (4.6)	3350 (25.3)	2090 (15.6)	-	This study
Manchester, UK	urban	winter	29 (2.1)	52 (3.7)	110 (7.8)	-	(Gabey et al., 2011)
Puy de Dôme mountain, France	high-altitude	summer	12 (4.4)	-	95 (35.2)	-	(Gabey et al., 2013)
Killarney, Ireland	rural	summer	175 (0.5)	95 (0.3)	35 (0.1)	15 (0.05)[a]	(Healy et al., 2014)
Borneo, Malaysis	rainforest	summer	-	-	-	150 [b]	(Gabey et al., 2010)
Karlsruhe, Germany	semi-rural	one year	-	-	-	31 (7.3) [b]	(Toprak and Schnaiter, 2013)
Amazon, Brazil	rainforest	spring	-	-	-	93 (26.3) [a]	(Huffman et al., 2012)
Mainz, Germany	semi-urban	summer, autumn, winter	-	-	-	27 (4) [a]	(Huffman et al., 2010)
Helsinki, Finland	urban	summer	-	-	-	13 (8) [a]	(Saari et al., 2015)
Hyytiälä, Finland	boreal forest	spring	-	-	-	15 (4.4) [a]	(Schumacher et al., 2013)
		summer	-	-	-	46 (13) [a]	
		autumn	-	-	-	27 (9.8) [a]	
		winter	-	-	-	4 (1.1) [a]	
Colorado, USA	rural	spring	-	-	-	15 (2.5) [a]	(Schumacher et al., 2013)
		summer	-	-	-	30 (8.8) [a]	
		autumn	-	-	-	17 (5.7) [a]	
		winter	-	-	-	5.3 (3) [a]	
Ghats, India	high-altitude	summer				20 (2)[a]	(Valsan et al., 2016)

a: results of UV-APS;

b: combine with FL1 and FL3 channel

Table 3. Integrated number concentrations (cm^{-3}) of each FAPs and fractions (%) of FAPs number concentrations to the total particle number concentration. Type AC is not listed.

Category	25th Percentile	Mean	Median	75th Percentile	Standard Deviation	Fraction
Type A	0.03	0.05	0.04	0.06	0.03	0.45
Type B	0.79	1.77	1.42	2.55	1.27	12.95
Type C	0.23	0.66	0.43	0.95	0.55	4.40
Type AB	0.07	0.15	0.11	0.18	0.12	1.20
Type BC	0.52	1.06	0.87	1.51	0.73	8.26
Type ABC	0.17	0.37	0.28	0.43	0.31	2.91
CR type	0.63	1.45	1.10	2.11	1.06	10.50
NCR type	0.32	0.64	0.54	0.83	0.46	4.69

Figures

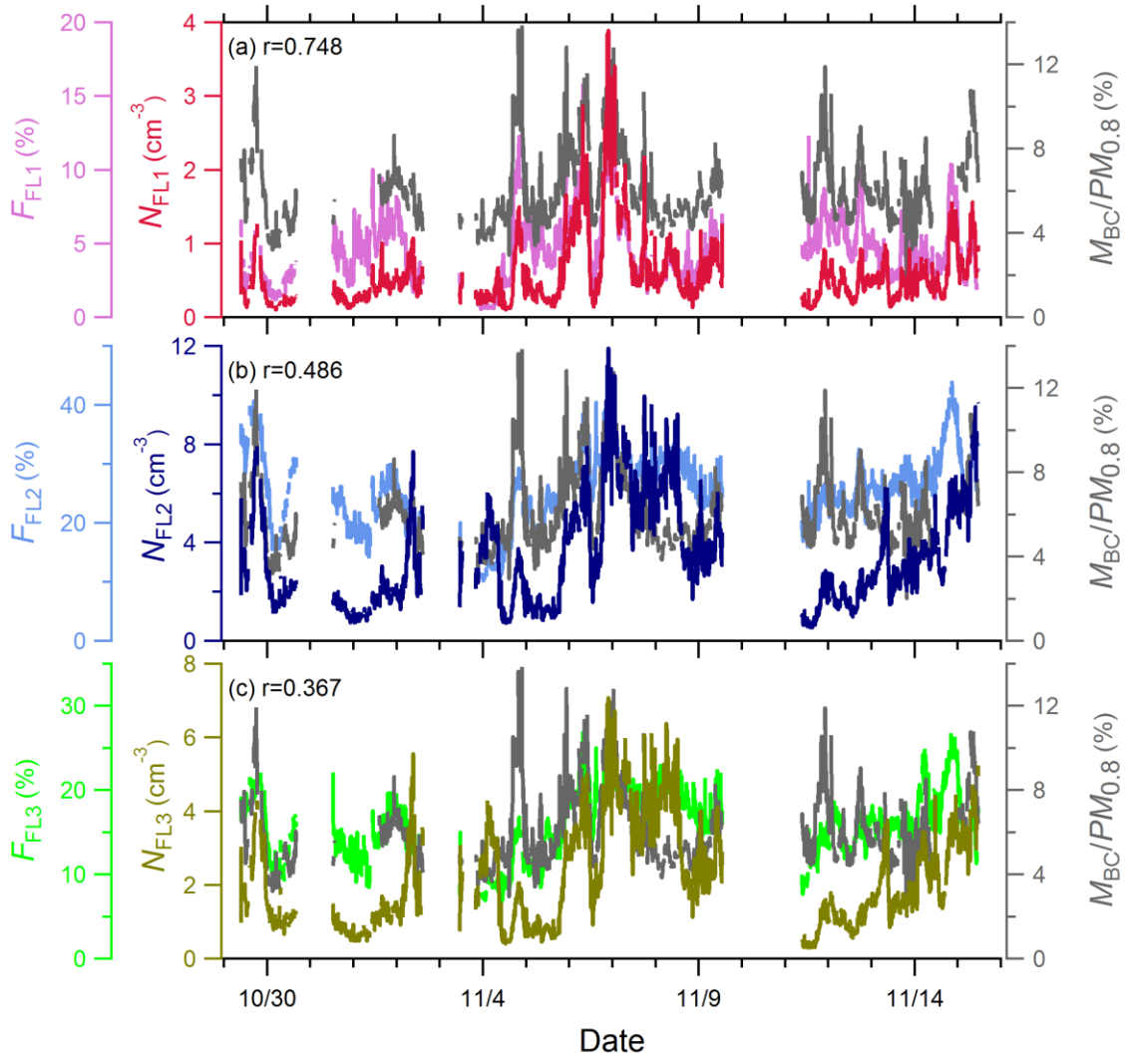

Figure 1. Time series of $M_{BC}/PM_{0.8}$ (gray line, right axis), number concentration of fluorescent particles in each channel (primary left axis) and relative number fractions of fluorescent particles in each channel (secondary left axis). (a) FL1 channel, $N_{FL1,}$ crimson line, F_{FL1}, orchid line. (b) FL2 channel, $N_{FL2,}$ navy line F_{FL2}, cornflower blue line. (c) FL3 channel, $N_{FL3,}$ olive line F_{FL3}, lime line. r is the correlation coefficient between F_x and $M_{BC}/PM_{0.8.}$

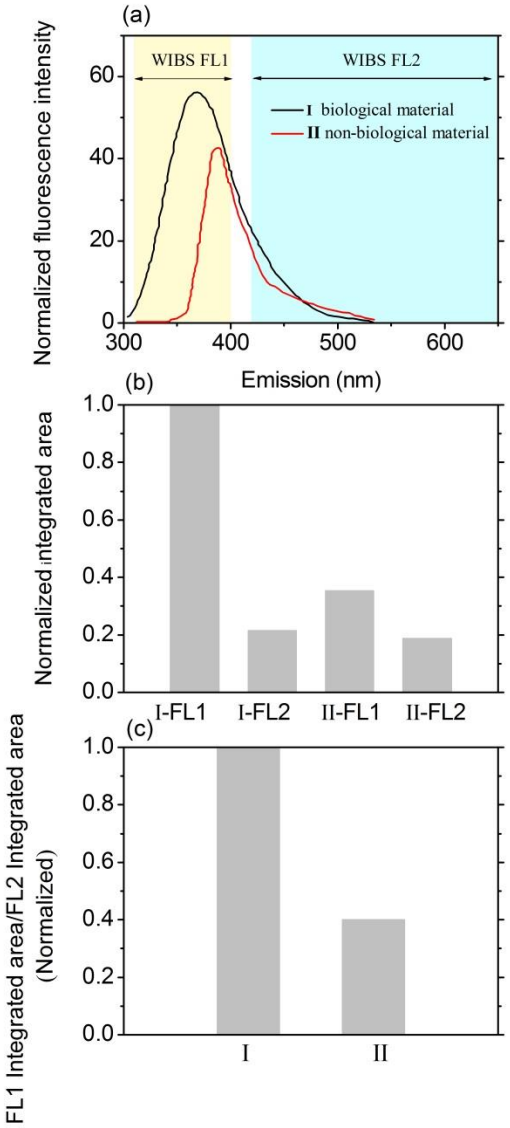

Figure 2. (a) Normalized fluorescence emission spectra of two fluorescent compounds: I (black line, biological material) and II (red line, non-biological material) for excitation wavelengths at λ_{ex}=280 nm. Shadow areas indicate the excitation wavebands of FL1 and FL2 channels of WIBS. (b) Integrated fluorescence intensity of two compounds in two bands (FL1 and FL2). (c) The ratio of fluorescence intensity from different WIBS channels (I_{FL1}/I_{FL2}) of I and II compounds. The fluorescence emission spectra are obtained from Pöhlker et al. (2012).

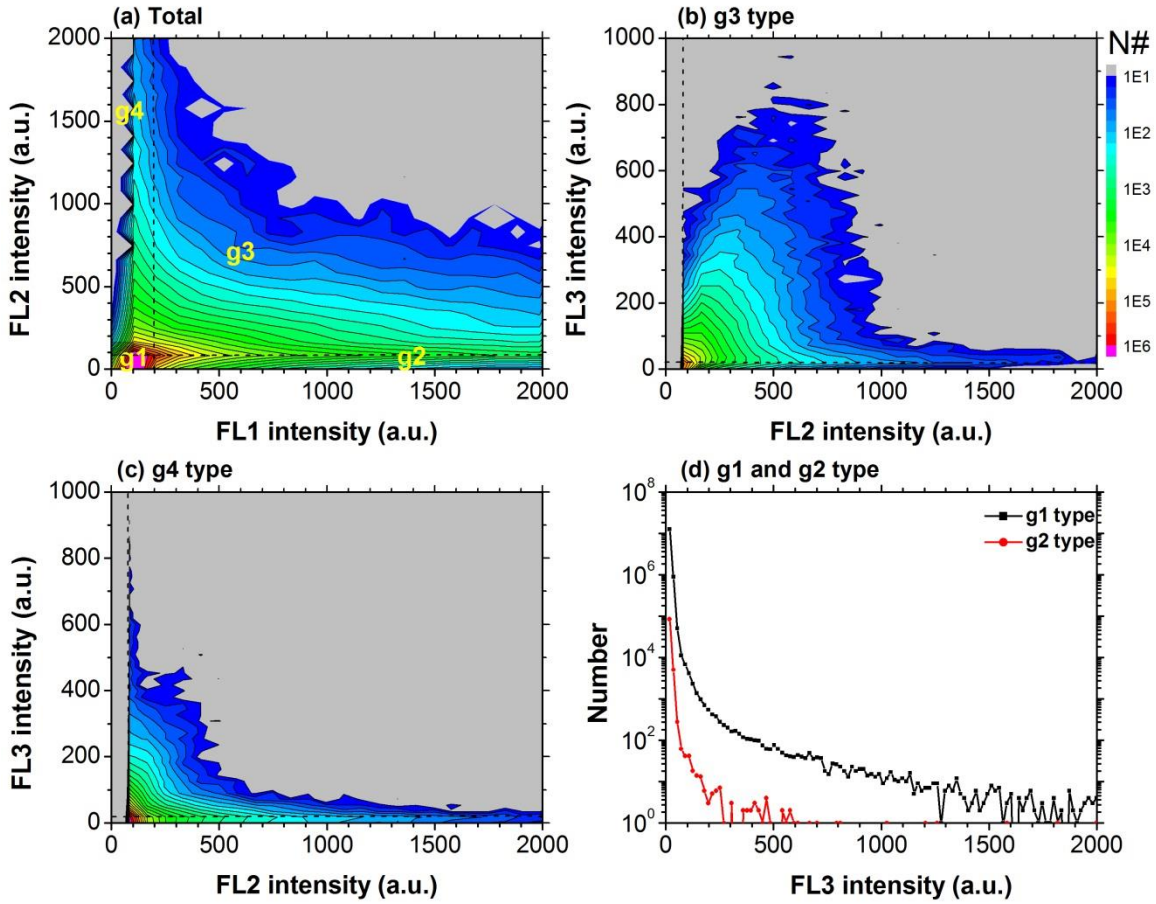

Figure 3. Spectral pattern of the classified fluorescence intensity. FL1 intensity is grouped at 100 intervals, FL2 intensity is grouped at 80 intervals and FL3 intensity is grouped at 18 intervals. Color scale is measured particle number. None fluorescent and saturating (FL⩾2000 a.u.) aerosol particles were excluded. (a) FL1 intensity versus FL2 intensity of total measured particles; (b) FL2 intensity versus FL3 intensity of g3 type particles; (c) FL2 intensity versus FL3 intensity of g4 type particles; (d) Numbers of g1 and g2 type particles of FL3 fluorescence intensity. Because FL2 intensity of g1 and g2 are below the threshold, the spectral patterns are hence not used. Dotted lines denote the threshold of each channel (200 a.u. for FL1, 80 a.u. for FL2 and 18 a.u. for FL3).

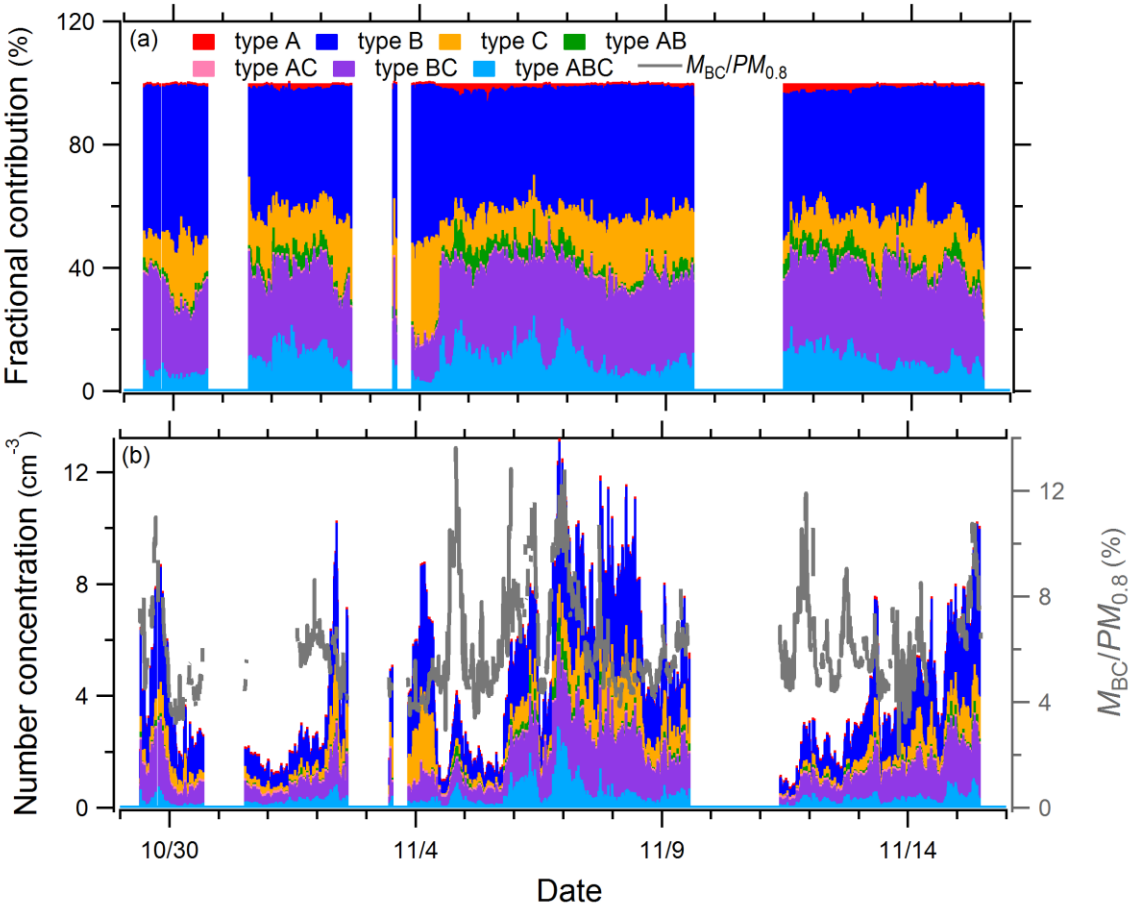

Figure 4. Time series of (a) the fractional contributions of each fluorescent type to the total FAPs and (b) number concentration (left axis) of each fluorescent type and $M_{BC}/PM_{0.8}$ (gray line, right axis). Red color indicate type A, blue color indicate type B, dark yellow indicate type C, green color indicate type AB, pink color indicate type AC, purple color indicate type BC, light blue color indicate type ABC.

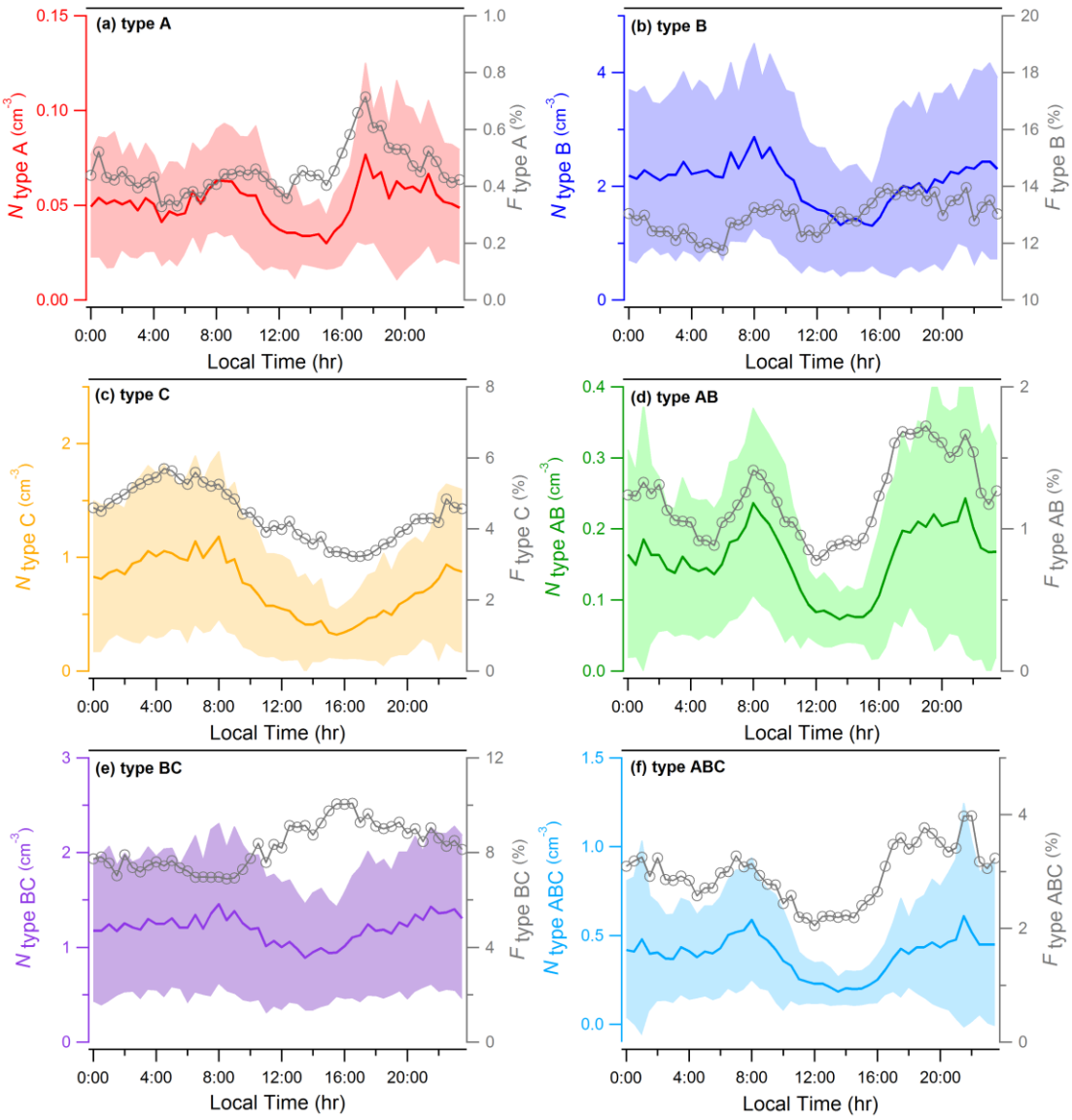

Figure 5. Diurnal variations of number concentrations of (a) type A, red, (b) type B, blue, (c) type C, dark yellow, (d) type AB, green, (e) type BC, purple and (f) type ABC, light blue. Gray line indicates the number fraction of respective fluorescent particles (right axis). Shading indicates ± one standard deviation.

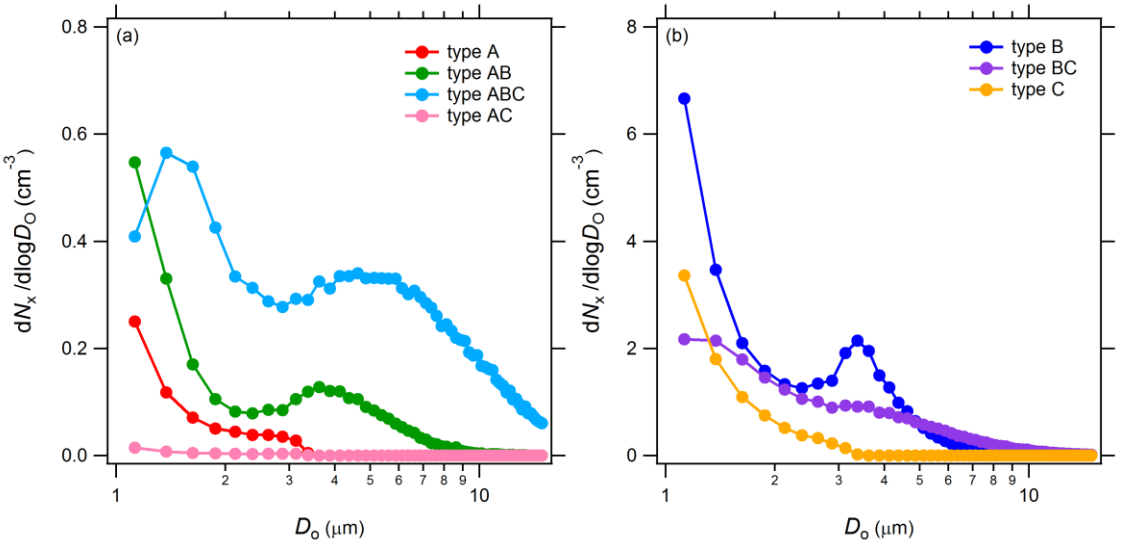

534

535 **Figure 6.** Mean number size distributions of (a) type A (red), type AB (green), type AC
536 (pink) and type ABC (light blue); (b) type B (blue), type BC (purple) and type C (dark
537 yellow).

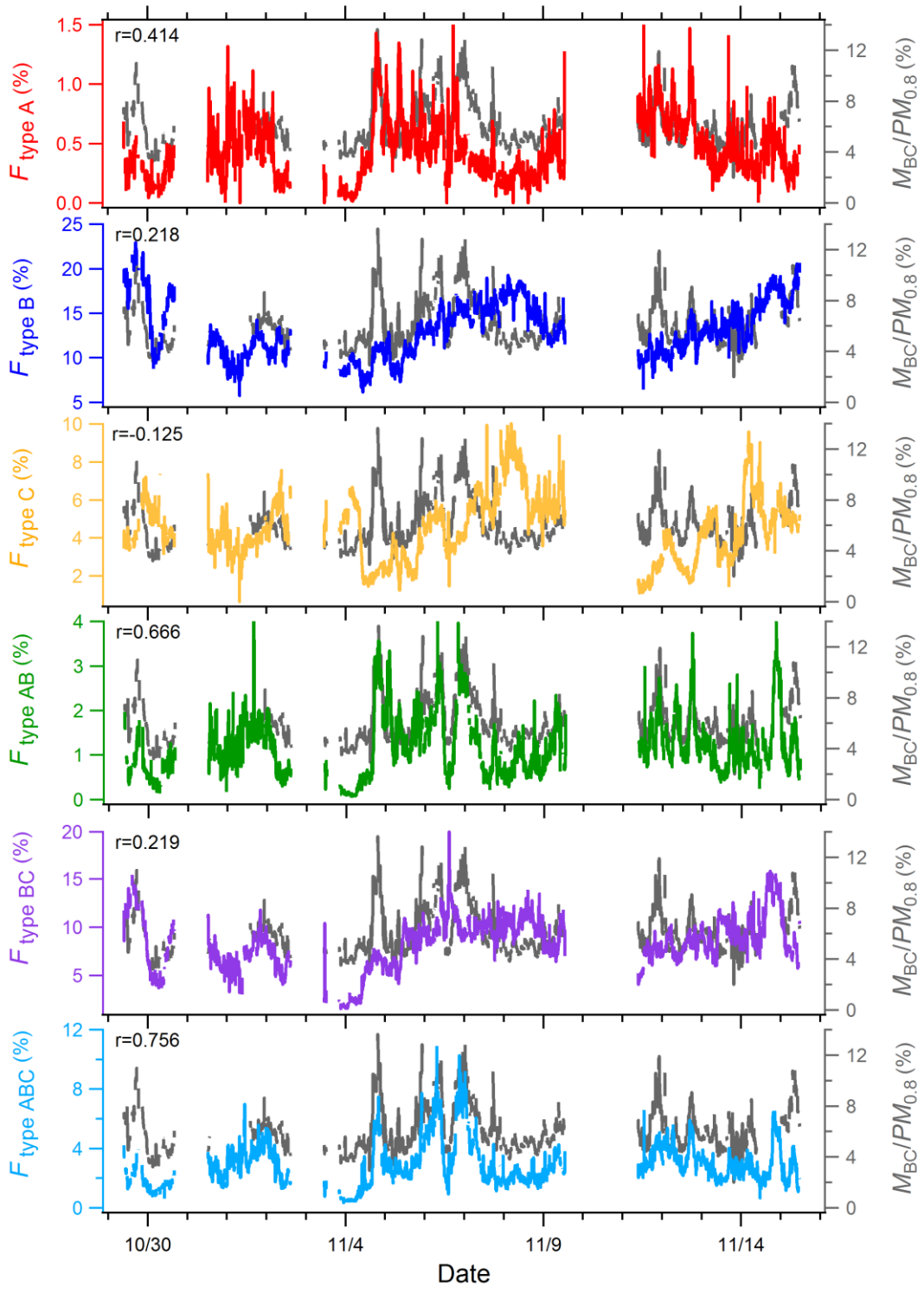

Figure 7. Time series of number fractions of various fluorescent particles (left axis) and $M_{BC}/PM_{0.8}$ (gray line, right axis). r is the correlation coefficient between F_x and $M_{BC}/PM_{0.8}$.

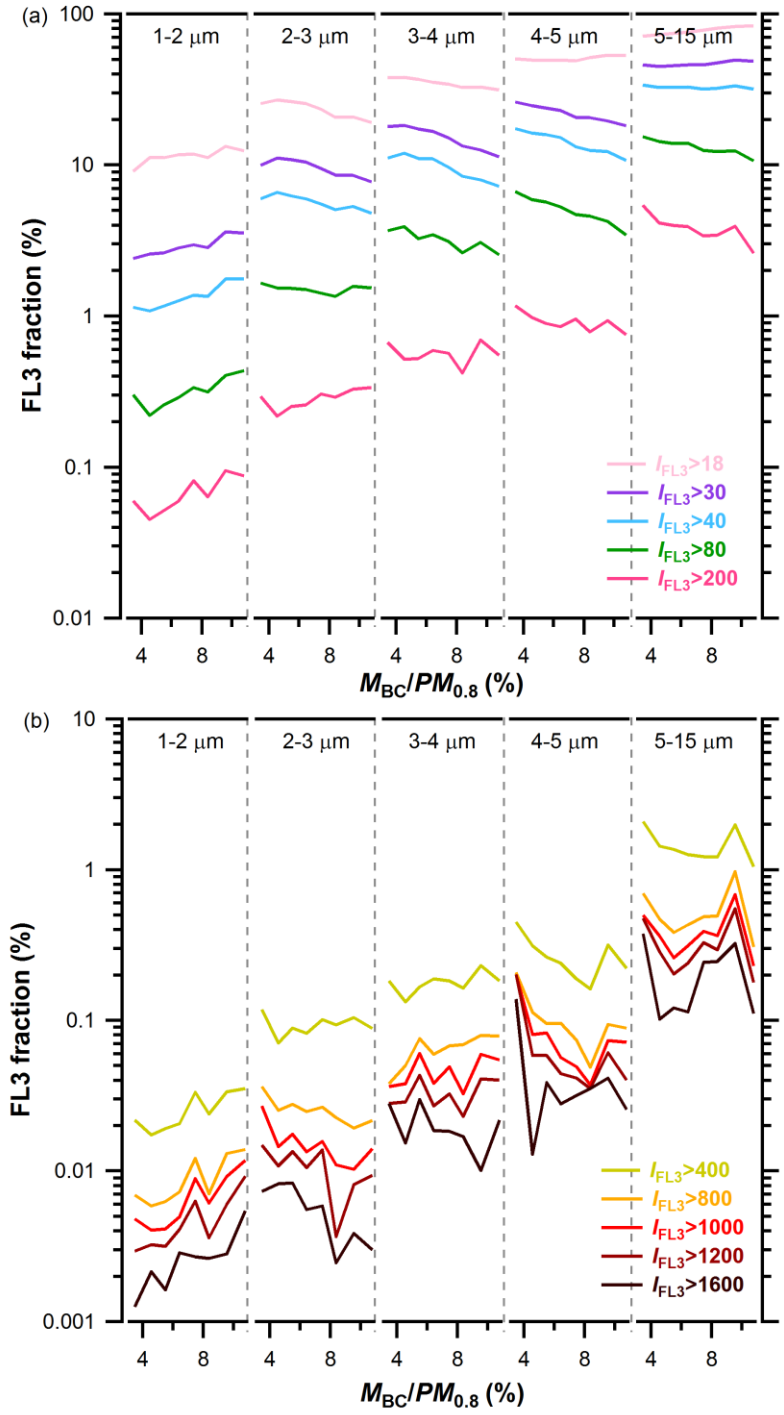

543

544 **Figure 8.** Correlations of FL3 fractions with $M_{BC}/PM_{0.8}$ in different size ranges. FL3
545 fraction is the number concentration of the subgroup ratio to the number concentration of
546 total particles in each size bin. (a) Low fluorescent intensity group. (b) High fluorescent
547 intensity group. The color lines represent the FL3 intensity (I_{FL3}) above the certain I_{cri}.

References

Brosseau, L. M., Vesley, D., Rice, N., Goodell, K., Nellis, M., and Hairston, P.: Differences in Detected Fluorescence Among Several Bacterial Species Measured with a Direct-Reading Particle Sizer and Fluorescence Detector, Aerosol Sci. Technol., 32, 545-558, 10.1080/027868200303461, 2000.

Gabey, A. M., Stanley, W. R., Gallagher, M. W., and Kaye, P. H.: The fluorescence properties of aerosol larger than 0.8 μm in urban and tropical rainforest locations, Atmos. Chem. Phys., 11, 5491-5504, 10.5194/acp-11-5491-2011, 2011.

Healy, D. A., Huffman, J. A., O'Connor, D. J., Pöhlker, C., Pöschl, U., and Sodeau, J. R.: Ambient measurements of biological aerosol particles near Killarney, Ireland: a comparison between real-time fluorescence and microscopy techniques, Atmos. Chem. Phys., 14, 8055-8069, 10.5194/acp-14-8055-2014, 2014.

Huffman, J. A., Sinha, B., Garland, R. M., Snee-Pollmann, A., Gunthe, S. S., Artaxo, P., Martin, S. T., Andreae, M. O., and Pöschl, U.: Size distributions and temporal variations of biological aerosol particles in the Amazon rainforest characterized by microscopy and real-time UV-APS fluorescence techniques during AMAZE-08, Atmos. Chem. Phys., 12, 11997-12019, 10.5194/acp-12-11997-2012, 2012.

Hungershoefer, K., et al.: Modelling the optical properties of fresh biomass burning aerosol produced in a smoke chamber: results from the EFEU campaign, Atmos. Chem. Phys., 8, 3427-3439, 10.5194/acp-8-3427-2008, 2008.

Miyakawa, T., Kanaya, Y., Taketani, F., Tabaru, M., Sugimoto, N., Ozawa, Y., and Takegawa, N.: Ground-based measurement of fluorescent aerosol particles in Tokyo in the spring of 2013: Potential impacts of nonbiological materials on autofluorescence measurements of airborne particles, J. Geophys. Res. Atmos., 120, 1171-1185, 10.1002/2014jd022189, 2015.

Morawska, L., Bofinger, N. D., Kocis, L., and Nwankwoala, A.: Submicrometer and Supermicrometer Particles from Diesel Vehicle Emissions, Environ Sci Technol, 32, 2033-2042, 10.1021/es970826+, 1998.

Oliver, J. D.: The viable but nonculturable state in bacteria, J Microbiol, 43, 93-100, 2005.

Pan, Y.-L., Pinnick, R. G., Hill, S. C., and Chang, R. K.: Particle-Fluorescence Spectrometer for Real-Time Single-Particle Measurements of Atmospheric Organic Carbon and Biological Aerosol, Environ. Sci. Technol., 43, 429-434, 10.1021/es801544y, 2009.

Pöhlker, C., Huffman, J. A., and Pöschl, U.: Autofluorescence of atmospheric bioaerosols – fluorescent biomolecules and potential interferences, Atmos. Meas. Tech., 5, 37-71, 10.5194/amt-5-37-2012, 2012.

Taketani, F., Kanaya, Y., Nakamura, T., Koizumi, K., Moteki, N., and Takegawa, N.: Measurement of fluorescence spectra from atmospheric single submicron particle using laser-induced fluorescence technique, J. Aerosol Sci., 58, 1-8, http://dx.doi.org/10.1016/j.jaerosci.2012.12.002, 2013.

Wei, K., Zheng, Y., Li, J., Shen, F., Zou, Z., Fan, H., Li, X., Wu, C.-y., and Yao, M.: Microbial aerosol characteristics in highly polluted and near-pristine environments featuring different climatic conditions, Science Bulletin, 60, 1439-1447, 10.1007/s11434-015-0868-y, 2015.